Chapter 4

An Efficient Temporal Approximation for Weakly Singular Time-Fractional Nonlinear Diffusion-Wave Equation with Variable Coefficients

This chapter deals with an efficient discretization in handling the discontinuous initial data and nonsmooth exact solution of the nonlinear TFDW equation with variable coefficients to achieve the optimal convergence rate. The nonuniform $L1$ approach with half point discretization process used to obtain the approximation of Caputo fractional derivative of order $\alpha \in (1, 2)$. The error analysis in approximation of the Caputo derivative is proved. Then the mentioned model is transformed into

a system of equations by using the developed nonuniform $L1$ method and second order approximation of the space derivatives. We constructed two linearized finite difference schemes in solving nonlinear single-term and multi-term TFDW equations with $\min(3-\alpha, \gamma(\alpha-1))$ and $\min(3-\alpha_r, \gamma(\alpha_r-1))$, $r = 0,\ 1,\ 2$ convergence order, respectively where parameter $\gamma \geq 1$ is used in formation of nonuniform temporal grids. The Von Neumann stability analysis is proved for the developed scheme. To illustrate the theoretical findings, we provided four numerical examples.

4.1 Introduction

The main motive of this chapter, we examined and elaborated an efficient approximation method in solving the nonlinear TFDW equation with variable coefficients:

$$ {}^{C}\mathcal{D}^{\alpha}_{0,t}u(x,t) + q(x)F(u(x,t)) = \frac{\partial}{\partial x}\left(p(x)\ \frac{\partial u(x,t)}{\partial x}\right) + f(x,t), \quad x \in \Omega,\ 0 < t \leq T, \tag{4.1} $$

$$ u(x,0) = \phi(x), \quad u_t(x,0) = \varphi(x), \quad x \in \overline{\Omega}(\equiv \Omega \cup \partial\Omega), \tag{4.2} $$

$$ u(x,t) = \Phi(x,t), \qquad x \in \partial\Omega,\ t \in (0,T], \tag{4.3} $$

where $\Omega = (0,L)$, $p \in C^1(\overline{\Omega})$, $q \in C(\overline{\Omega})$, $0 < c_1 \leq p(x) \leq c_2$, $q(x) \geq 0$, $\forall x \in \overline{\Omega}$, $\phi \in C(\overline{\Omega})$, $\varphi \in C(\overline{\Omega})$, $\Phi \in C(\overline{\Omega} \times [0,T])$, $f \in C(\overline{\Omega} \times [0,T])$, where the function $F(u)$ satisfies the Lipschitz condition with Lipschitz constant $\mathcal{L}$ i.e.

$$ |F(u) - F(\widehat{u})| \leq \mathcal{L}|u - \widehat{u}|, \quad \forall\ u,\ \widehat{u}, \tag{4.4} $$

and the operator ${}^{C}\mathcal{D}_{0,t}^{\alpha}$ denotes the Caputo fractional derivative of order $\alpha \in (1,2)$, which is defined as [12, 14]:

$$ {}^{C}\mathcal{D}_{0,t}^{\alpha} u(x,t) = \frac{1}{\Gamma(2-\alpha)} \int_0^t (t-s)^{1-\alpha} \frac{\partial^2 u(x,s)}{\partial s^2}\, ds. \tag{4.5} $$

The primary objective of this chapter is to handle the discontinuous initial data and nonsmooth exact solutions of the variable coefficients nonlinear TFDW equation. We involved the nonuniform temporal discretization of the time domain to tackle the initial singularity $t = 0$ in nonsmooth solutions of problem (4.1)-(4.3). Moreover, in the existing literature [73, 79, 127, 128, 129] authors proposed the numerical schemes in solving the constant coefficients linear and nonlinear TFDW equations with some specific regularity conditions. The key contribution of the proposed chapter consists of the followings:

- We proposed and analyzed two difference schemes to solve the one-dimensional Klein-Gordon and Sine-Gordon single-term and multi-term TFDW equations with variable coefficients. For the numerical solutions of the two-dimensional Klein-Gordon and Sine-Gordon TFDW equations with variable coefficients, we use linearized alternating direction implicit approach with half point discretization of Caputo derivative of order $\alpha \in (1,2)$ on nonuniform meshes.

- The analysis of error bound in approximating the Caputo derivative is demonstrated by assuming weak initial singularity at $t = 0$.

- Considering the graded temporal meshes and under some weak regularity conditions on exact solutions of nonlinear TFDW problem, the established difference schemes are $\mathcal{O}(N^{-\min(3-\alpha,\gamma\alpha)} + h^2)$ and $\mathcal{O}(N^{-\min(3-\alpha_r,\gamma\alpha_r)} + h^2)$-order accurate.

- To demonstrate the effectiveness of nonuniform finite difference schemes, we perform four computational experiments involving nonsmooth exact solutions, incorporating discontinuous initial conditions and quantify the solution behavior near singularity point $t = 0$ through absolute error figures.

The structure of the chapter is organized in the following manner: In Section 4.2, we examine the discretization of the Caputo fractional derivative of order $\alpha \in (1, 2)$ on nonuniform temporal meshes and also establish error bound of the Caputo derivative approximation. In Section 4.3, we propose two linearized finite difference schemes in solving the single-term and multi-term TFDW equations, and discuss ADI scheme for the numerical solution of two-dimensional model. In Section 4.4, we examine the unconditional stability analysis of the approximation scheme. In Section 4.5, we display numerical examples involving both smooth and nonsmooth exact solutions having discontinuous initial conditions to confirm the theoretical convergence rate. A concise summary of the work is provided in Section 4.6.

Throughout this chapter, symbol C represents a positive generic constant that is independent from time and space step-sizes, initial data $u|_{t=0}$, source function f. However, it may depend on the parameter α and time T.

4.2 Time-Stepping Discretization of Caputo Derivative on Nonuniform Mesh

Consider the partition of the interval $[0, T]$ then the nonuniform temporal grids domain is $\Omega_\tau = \{t_n | t_n = \left(\frac{n}{N}\right)^\gamma T : \ \gamma \geq 1, \ 1 \leq n \leq N-1\}$ with $\overline{\Omega}_\tau = \Omega_\tau \cup \partial\Omega_\tau$. The time step sizes are $\tau_n = t_n - t_{n-1}$ with the assumption $0 \leq \tau_{n-1} \leq \tau_n$, $1 \leq n \leq N$. We construct the temporal nodes $t_k = (k\tau)^\gamma$, $0 \leq k \leq n$, where $\gamma \geq 1$ used to

accumulate the nodes near $t = 0$ by increasing the value of γ, and $\tau = \frac{T^{\frac{1}{\gamma}}}{N}$. The fractional grids are followed by using $t_{n-\lambda} = \lambda t_{n-1} + (1-\lambda)t_n$, $0 \leq \lambda \leq 1$. Suppose $v(t) = \frac{\partial u}{\partial t}(t)$ and $\mathcal{F}_t = \{g(t_n) = g^n | 1 \leq n \leq N\}$. Then, we define some notations on grids as:

$$
\begin{aligned}
u^{k+\frac{1}{2}} &= \frac{u^{k+1} + u^k}{2}, \\
\implies \left.\frac{\partial u(t)}{\partial t}\right|_{t=t_{k+\frac{1}{2}}} &= \frac{u^{k+1} - u^k}{\tau_{k+1}} + \mathcal{R}_1^{k+\frac{1}{2}}, \ k = 0, 1, ..., N-1, \qquad (4.6) \\
\left.\frac{\partial v(t)}{\partial t}\right|_{t=t_{k+\frac{1}{2}}} &= \frac{4}{(\tau_{k+2} + 2\tau_{k+1} + \tau_k)} \left[\frac{u^{k+\frac{3}{2}} - u^{k+\frac{1}{2}}}{t_{k+\frac{3}{2}} - t_{k+\frac{1}{2}}} - \frac{u^{k+\frac{1}{2}} - u^{k-\frac{1}{2}}}{t_{k+\frac{1}{2}} - t_{k-\frac{1}{2}}}\right] + \mathcal{R}_2^{k+\frac{1}{2}}, \qquad (4.7)
\end{aligned}
$$

where

$$
\begin{aligned}
\left|\mathcal{R}_1^{k+\frac{1}{2}}\right| &\leq \frac{1}{2!\tau_{k+1}} \left[\int_{t_k}^{t_{k+\frac{1}{2}}} (t - t_k)^2 u'''(t) dt + \int_{t_{k+\frac{1}{2}}}^{t_{k+1}} (t_{k+1} - t)^2 u'''(t) dt\right], \qquad (4.8) \\
\left|\mathcal{R}_2^{k+\frac{1}{2}}\right| &\leq \frac{4}{3!(\tau_{k+2} + 2\tau_{k+1} + \tau_k)} \left|\left[\frac{1}{t_{k+\frac{1}{2}} - t_{k-\frac{1}{2}}} \int_{t_{k-\frac{1}{2}}}^{t_{k+\frac{1}{2}}} (t - t_{k-\frac{1}{2}})^3 u''''(t) dt \right.\right. \\
&\qquad \left.\left. - \frac{1}{t_{k+\frac{3}{2}} - t_{k+\frac{1}{2}}} \int_{t_{k+\frac{1}{2}}}^{t_{k+\frac{3}{2}}} (t_{k+\frac{3}{2}} - t)^3 u''''(t) dt\right]\right| \qquad (4.9)
\end{aligned}
$$

(R1) Consequentially to [108], we assume that the unique solution u of (4.1) holds the following bound for all $t \in (0, T]$, where C is a constant:

$$
u(., t) \in C^2[0, T] \cap C^3(0, T], \quad \left|\frac{\partial^k u(t)}{\partial t^k}\right| \leq C\big(1 + t^{\alpha - k}\big), \quad k = 0, 1, 2, 3. \qquad (4.10)
$$

(R2) The considered temporal step-sizes satisfies the following inequality

$$
\begin{aligned}
&2^{-\gamma} t_{m+1} \leq t_m, \quad m = 1, 2, ..., n-1, \ 1 \leq n \leq N. \\
&\frac{t_{m+1}}{t_m} = \left(\frac{m+1}{m}\right)^{\gamma} = (1 + \frac{1}{m})^{\gamma} \leq 2^{\gamma}. \qquad (4.11)
\end{aligned}
$$

(R3) The following bound will be useful to show the theoretical analysis for the discretization scheme in solving the problem (4.1)-(4.3):

$$\begin{aligned}\tau_m &= T\left[\left(\frac{m}{N}\right)^{\gamma} - \left(\frac{m-1}{N}\right)^{\gamma}\right], \quad 1 \le m \le n-1, \ 1 \le n \le N,\\ &= TN^{-\gamma}m^{\gamma}\left[1 - \left(1 - \frac{1}{m}\right)^{\gamma}\right] \le CTN^{-\gamma}m^{\gamma-1}. \end{aligned} \tag{4.12}$$

(R4) If $\Xi_m = \frac{\tau_{m+1}}{\tau_m}$, $1 \le m \le n-1$, $1 \le n \le N$, then $1 < \Xi_{m+1} \le \Xi_m$.

Since, $\tau_{m+1} = T[(m+1)^{\gamma} - m^{\gamma}]N^{-\gamma}$, then there exist $\theta \in (0,1)$ such that

$$\frac{\tau_{m+1}}{\tau_m} = \frac{(m+1)^{\gamma} - m^{\gamma}}{m^{\gamma} - (m-1)^{\gamma}} = \frac{(m+\theta)^{\gamma-1}}{(m-1+\theta)^{\gamma-1}} \ge \left(1 + \frac{1}{m}\right)^{\gamma-1} > 1.$$

Similarly, $\frac{\tau_{m+2}}{\tau_{m+1}} = \frac{(m+1+\theta)^{\gamma-1}}{(m+\theta)^{\gamma-1}} \le \left(1 + \frac{1}{m}\right)^{\gamma-1} \le \Xi_m$.

In Figure 4.1, we illustrate the development of the step size τ_n over the time domain $[0, T]$ with increasing the values of parameter γ. This demonstrates the variable step sizes accumulate more near $t = 0$ as we increase the values of γ.

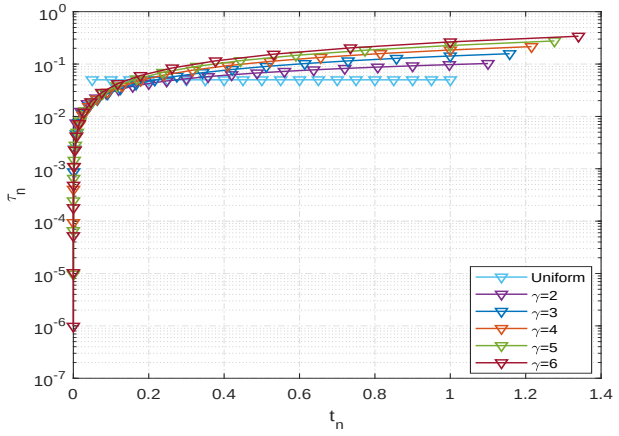

FIGURE 4.1: The change in variable step sizes τ_n is analyzed for several different values of parameter γ.

The half-point discretization of Caputo derivative ${}^{C}\mathcal{D}_{0,t}^{\alpha-1}v(t)$, $1<\alpha<2$ at the grid t_n is given as follows:

$$
\begin{aligned}
{}^{C}\mathcal{D}_{0,t}^{\alpha-1}v(t_n) = \frac{1}{\Gamma(2-\alpha)}\Bigg[\sum_{m=0}^{n-1}\int_{t_{m-\frac{1}{2}}}^{t_{m+\frac{1}{2}}}(t_n-\mathfrak{p})^{-\alpha}\,\frac{\partial v(\mathfrak{p})}{\partial \mathfrak{p}}d\mathfrak{p} \\
+\int_{t_{n-\frac{1}{2}}}^{t_n}(t_n-\mathfrak{p})^{-\alpha}\,\frac{\partial v(\mathfrak{p})}{\partial \mathfrak{p}}d\mathfrak{p}-\int_{t_{-\frac{1}{2}}}^{t_0}(t_n-\mathfrak{p})^{-\alpha}\,\frac{\partial v(\mathfrak{p})}{\partial \mathfrak{p}}d\mathfrak{p}\Bigg]. \qquad (4.13)
\end{aligned}
$$

- We consider linear interpolation polynomial using points $\{(t_{m-\frac{1}{2}}, v(t)|_{t_{m-\frac{1}{2}}}),\ (t_{m+\frac{1}{2}}, v(t)|_{t_{m+\frac{1}{2}}})\}$, $0\le m\le n-1$ and $\{(t_{n-\frac{3}{2}}, v(t)|_{t_{n-\frac{3}{2}}}), (t_{n-\frac{1}{2}}, v(t)|_{t_{n-\frac{1}{2}}})\}$, $n\ge 1$ to approximate the $\frac{\partial v(t)}{\partial t}$ in first and second integration terms of (4.13), respectively with $t_{-\frac{1}{2}}=t_0$. Then, we observe that $v(t)|_{t_{-\frac{1}{2}}}=v(t_0)+\mathcal{O}(\tau_n^2)$ (see [130]).

In accordance with the method discussed in [130], the approximate formula of Caputo derivative at t_n is:

$$
\begin{aligned}
&{}^{C}\mathcal{D}_{0,t}^{\alpha}u(t)|_{t_n} \\
&=\frac{1}{\Gamma(2-\alpha)}\Bigg[\sum_{m=0}^{n-1}\left\{\frac{v^{m+\frac{1}{2}}-v^{m-\frac{1}{2}}}{t_{m+\frac{1}{2}}-t_{m-\frac{1}{2}}}\right\}\int_{t_{m-\frac{1}{2}}}^{t_{m+\frac{1}{2}}}(t_n-\mathfrak{p})^{1-\alpha}d\mathfrak{p}+\varepsilon_1^{(\alpha)} \\
&\quad+\left\{\frac{v^{n-\frac{1}{2}}-v^{n-\frac{3}{2}}}{t_{n-\frac{1}{2}}-t_{n-\frac{3}{2}}}\right\}\int_{n-\frac{1}{2}}^{t_n}(t_n-\mathfrak{p})^{1-\alpha}d\mathfrak{p}+\varepsilon_2^{(\alpha)}\Bigg], \\
&=\frac{2}{\Gamma(3-\alpha)}\Bigg[\sum_{m=0}^{n-1}\frac{[(t_n-t_{m-\frac{1}{2}})^{2-\alpha}-(t_n-t_{m+\frac{1}{2}})^{2-\alpha}]}{(\tau_m+\tau_{m+1})}\left\{\frac{(u^{m+1}-u^m)}{\tau_{m+1}}-\frac{(u^m-u^{m-1})}{\tau_m}\right\} \\
&\quad+\frac{1}{(\tau_{n-1}+\tau_n)}\left(\frac{\tau_n}{2}\right)^{2-\alpha}\left\{\frac{(u^n-u^{n-1})}{\tau_n}-\frac{(u^{n-1}-u^{n-2})}{\tau_{n-1}}\right\}\Bigg]+\mathcal{R}_t^{(\alpha)}+\widehat{\mathcal{R}}_1^n, \\
&=\frac{2}{\Gamma(3-\alpha)}\Bigg[\sum_{m=0}^{n-1}\mathcal{C}_{n,m}^{(\alpha)}\frac{(u^{m+1}-u^m)}{\tau_{m+1}}-\sum_{m=1}^{n-1}\mathcal{C}_{n,m}^{(\alpha)}\frac{(u^m-u^{m-1})}{\tau_m} \\
&\quad+\mathcal{S}(n)\left\{\frac{(u^n-u^{n-1})}{\tau_n}-\frac{(u^{n-1}-u^{n-2})}{\tau_{n-1}}\right\}\Bigg]+\mathcal{R}_t^{(\alpha)}+\widehat{\mathcal{R}}_1^n, \\
&=\frac{2}{\Gamma(3-\alpha)}\Bigg[\left(\frac{\mathcal{C}_{n,n-1}^{(\alpha)}+\mathcal{S}(n)}{\tau_n}\right)(u^n-u^{n-1})-\frac{\mathcal{S}(n)}{\tau_{n-1}}(u^{n-1}-u^{n-2})
\end{aligned}
$$

$$+\sum_{m=1}^{n-1}\left(\frac{\mathcal{C}_{n,m-1}^{(\alpha)}-\mathcal{C}_{n,m}^{(\alpha)}}{\tau_m}\right)(u^m-u^{m-1})\Big]+\mathcal{R}_t^{(\alpha)}+\widehat{\mathcal{R}}_1^n$$

$$=_0\partial_t^\alpha u(t_n)+\mathcal{R}_t^{(\alpha)}, \tag{4.14}$$

where $\mathcal{R}_t^{(\alpha)}=\varepsilon_1^{(\alpha)}+\varepsilon_2^{(\alpha)}$, and

$$|\widehat{\mathcal{R}}_1^n|\leq\frac{2}{\Gamma(3-\alpha)}\left|\left[\sum_{m=0}^{n-1}\mathcal{C}_{n,m}^{(\alpha)}\big(\mathcal{R}_1^{m+1/2}-\mathcal{R}_1^{m-1/2}\big)+\mathcal{S}(n)(\mathcal{R}_1^{n-\frac{1}{2}}-\mathcal{R}_1^{n-\frac{3}{2}})\right]\right|,\quad n\geq 1. \tag{4.15}$$

For $n\geq 1$, $1\leq m\leq n-1$, the corresponding coefficients of equation (4.14) are given as:

$$\mathcal{C}_{n,0}^{(\alpha)}=\frac{1}{\tau_1}\big[(t_n-t_0)^{2-\alpha}-2^{\alpha-2}(2t_n-t_0-t_1)^{2-\alpha}\big], \tag{4.16}$$

$$\mathcal{C}_{n,m}^{(\alpha)}=\frac{[(t_n-t_{m-\frac{1}{2}})^{2-\alpha}-(t_n-t_{m+\frac{1}{2}})^{2-\alpha}]}{\tau_m+\tau_{m+1}}, \tag{4.17}$$

$$\mathcal{S}(n)=2^{\alpha-2}\frac{\tau_n^{2-\alpha}}{\tau_n+\tau_{n-1}},\qquad n\geq 1. \tag{4.18}$$

We can easily establish the following bound using Mean Value Theorem

$$0\leq\mathcal{C}_{n,m}^{(\alpha)}\leq\mathcal{C}_{n,m+1}^{(\alpha)},\quad n\geq 1,\ m\geq 0, \tag{4.19}$$

and for positive constants C_1, C_2, one has

$$C_1(t_n-t_{m+\frac{1}{2}})^{1-\alpha}\leq\mathcal{C}_{n,m}^{(\alpha)}\leq C_2(t_n-t_{m-\frac{1}{2}})^{1-\alpha},\quad 0\leq m\leq n-1,\quad n\geq 1. \tag{4.20}$$

Since ${}_0\mathcal{D}_t^\alpha u(t_n)-{}_0\partial_t^\alpha u(t_n)=\mathcal{R}_t^{(\alpha)}$ for $n\in\{1,2,...,N\}$ with $\mathcal{R}_t^{(\alpha)}=\varepsilon_1^{(\alpha)}+\varepsilon_2^{(\alpha)}$, where

$$\varepsilon_1^{(\alpha)}=\frac{1}{\Gamma(2-\alpha)}\sum_{m=0}^{n-1}\int_{m-\frac{1}{2}}^{t_{m+\frac{1}{2}}}(t_n-\mathfrak{p})^{1-\alpha}\left\{\frac{\partial v(\mathfrak{p})}{\partial\mathfrak{p}}-\frac{v^{m+\frac{1}{2}}-v^{m-\frac{1}{2}}}{t_{m+\frac{1}{2}}-t_{m-\frac{1}{2}}}\right\}d\mathfrak{p}, \tag{4.21}$$

$$\varepsilon_2^{(\alpha)} = \frac{1}{\Gamma(2-\alpha)} \int_{n-\frac{1}{2}}^{t_n} (t_n - \mathfrak{p})^{1-\alpha} \left\{ \frac{\partial v(\mathfrak{p})}{\partial \mathfrak{p}} - \frac{v^{n-\frac{1}{2}} - v^{n-\frac{3}{2}}}{t_{n-\frac{1}{2}} - t_{n-\frac{3}{2}}} \right\} d\mathfrak{p}. \tag{4.22}$$

Using integration by parts in (4.21), we obtain

$$\begin{aligned}\varepsilon_1^{(\alpha)} =& \frac{1}{\Gamma(2-\alpha)} \sum_{m=0}^{n-1} \left\{ \left| (t_n - \mathfrak{p})^{1-\alpha} \left[v(\mathfrak{p}) - \frac{v^{m+\frac{1}{2}} - v^{m-\frac{1}{2}}}{t_{m+\frac{1}{2}} - t_{m-\frac{1}{2}}} (\mathfrak{p}) \right] \right|_{t_{m-\frac{1}{2}}}^{t_{m+\frac{1}{2}}} \right. \\ &\left. + \frac{(1-\alpha)}{\Gamma(2-\alpha)} \int_{t_{m-\frac{1}{2}}}^{t_{m+\frac{1}{2}}} (t_n - \mathfrak{p})^{-\alpha} \left(X(\mathfrak{p}) - Y(\mathfrak{p}) \right) d\mathfrak{p} \right\},\end{aligned}$$

where (by using the Mean Value Theorem)

$$\begin{aligned} X(\mathfrak{p}) &= v(\varpi) - v(t_{m-\frac{1}{2}}), \qquad \varpi \in (t_{m+\frac{1}{2}}, t_{m-\frac{1}{2}}), \\ Y(\mathfrak{p}) &= \frac{v^{m+\frac{1}{2}} - v^{m-\frac{1}{2}}}{t_{m+\frac{1}{2}} - t_{m-\frac{1}{2}}} (\varpi - t_{m-\frac{1}{2}}), \qquad \varpi \in (t_{m+\frac{1}{2}}, t_{m-\frac{1}{2}}), \end{aligned}$$

Now,

$$\begin{aligned} X(\mathfrak{p}) - Y(\mathfrak{p}) &= \frac{\left[v(\varpi) - v(t_{m-\frac{1}{2}}) \right]}{\varpi - t_{m-\frac{1}{2}}} (\varpi - t_{m-\frac{1}{2}}) - \frac{v^{m+\frac{1}{2}} - v^{m-\frac{1}{2}}}{t_{m+\frac{1}{2}} - t_{m-\frac{1}{2}}} (\varpi - t_{m-\frac{1}{2}}) \\ &= (\varpi - t_{m-\frac{1}{2}})(\varpi_1 - \varpi_2) \frac{\partial^2 v(\varpi_3)}{\partial t^2}, \quad \varpi_1,\ \varpi_2,\ \varpi_3 \in (t_{m+\frac{1}{2}}, t_{m-\frac{1}{2}}). \end{aligned}$$

Therefore, the equation (4.21) and (4.22) yields

$$\begin{aligned} |\varepsilon_1^{(\alpha)}| \leq \left| \frac{(1-\alpha)}{\Gamma(2-\alpha)} \sum_{m=0}^{n-1} \left[\left(t_{m+\frac{1}{2}} - t_{m-\frac{1}{2}} \right)^2 \right. \right. \\ \left. \left. \max_{t \in (t_{m-\frac{1}{2}},\ t_{m+\frac{1}{2}})} \left(\frac{\partial^2 v(t)}{\partial t^2} \right) \int_{t_{m-\frac{1}{2}}}^{t_{m+\frac{1}{2}}} (t_n - \mathfrak{p})^{-\alpha} d\mathfrak{p} \right] \right|, \end{aligned} \tag{4.23}$$

$$|\varepsilon_2^{(\alpha)}| \leq \left| \frac{(1-\alpha)}{\Gamma(2-\alpha)} \left(t_n - t_{n-\frac{1}{2}} \right)^2 \max_{t \in (t_{n-\frac{1}{2}},\ t_n)} \left(\frac{\partial^2 v(t)}{\partial t^2} \right) \int_{t_{n-\frac{1}{2}}}^{t_n} (t_n - \mathfrak{p})^{-\alpha} d\mathfrak{p} \right|. \tag{4.24}$$

4.2.1 Error Analysis

Lemma 4.2.1. For all $1 < \alpha < 2$ and $t \in (0, T]$, it holds

$$|{}^{C}\mathcal{D}^{\alpha}_{0,t} u(t_n) -_0 \partial^{\alpha}_t u(t_n)| \leq C\ n^{-\min\{(3-\alpha),\ \gamma(\alpha-1)\}}.$$

Proof. For $1 \leq m \leq n-1$. Using the inequality (4.10) into (4.23), we obtain

$$\begin{aligned}
|\varepsilon_1^{(\alpha)}| &\leq \left| \frac{(1-\alpha)}{\Gamma(2-\alpha)} \sum_{m=1}^{n-1} \left[\left(t_{m+\frac{1}{2}} - t_{m-\frac{1}{2}}\right)^2 \max_{t\in(t_{m-\frac{1}{2}},\ t_{m+\frac{1}{2}})} |u_{ttt}(t)| \int_{t_{m-\frac{1}{2}}}^{t_{m+\frac{1}{2}}} (t_n - \mathfrak{p})^{-\alpha} d\mathfrak{p} \right] \right| \\
&\leq C \sum_{m=1}^{n-1} \left[\left(t_{m+\frac{1}{2}} - t_{m-\frac{1}{2}}\right)^2 t_{m-\frac{1}{2}}^{\alpha-3} \int_{t_{m-\frac{1}{2}}}^{t_{m+\frac{1}{2}}} (t_n - \mathfrak{p})^{-\alpha} d\mathfrak{p} \right] \\
&\leq C \sum_{m=1}^{n-1} \left[\left(t_{m+\frac{1}{2}} - t_{m-\frac{1}{2}}\right)^2 t_{m-\frac{1}{2}}^{\alpha-3} \ (t_n - t_{m+\frac{1}{2}})^{-\alpha} \ (t_{m+\frac{1}{2}} - t_{m-\frac{1}{2}}) \right] \\
&\leq C \sum_{m=1}^{n-1} \left[\left(\frac{\tau_{m+1} + \tau_m}{2} \right)^3 \left(\frac{t_m + t_{m-1}}{2} \right)^{\alpha-3} \left(\frac{(t_n - t_{m+1}) + (t_n - t_m)}{2} \right)^{-\alpha} \right] \\
&\leq C \sum_{m=1}^{n-1} \left[\tau_{m+1}^3\ t_m^{\alpha-3}\ (t_n - t_m)^{-\alpha} \right]. \qquad (4.25)
\end{aligned}$$

For $1 \leq m \leq \lceil \frac{n}{2} \rceil - 1$, and using (4.12) into (4.25), we obtain

$$\begin{aligned}
|\varepsilon_1^{(\alpha)}| &\leq C \sum_{m=1}^{\lceil \frac{n}{2} \rceil - 1} \tau_{m+1}^3\ t_m^{\alpha-3}\ t_n^{-\alpha} \\
&\leq C \sum_{m=1}^{\lceil \frac{n}{2} \rceil - 1} \left\{ \left(TN^{-\gamma} m^{\gamma-1}\right)^3\ T^{\alpha-3} \left(\frac{m}{N}\right)^{\gamma(\alpha-3)}\ T^{-\alpha} \left(\frac{n}{N}\right)^{-\gamma\alpha} \right\} \\
&\leq C\ n^{-\gamma\alpha} \sum_{m=1}^{\lceil \frac{n}{2} \rceil - 1} m^{\gamma\alpha-3} := \begin{cases} C\ n^{-\gamma\alpha}\ ; & \gamma\alpha < 2, \\ C\ n^{-2}\ \ln(n)\ ; & \gamma\alpha = 2, \\ C\ n^{-2}\ ; & \gamma\alpha > 2. \end{cases} \qquad (4.26)
\end{aligned}$$

For $\lceil \frac{n}{2} \rceil \leq m < n-1$,

$$
\begin{aligned}
|\varepsilon_1^{(\alpha)}| &\leq C \sum_{m=\lceil \frac{n}{2} \rceil}^{n-1} \left\{ \tau_{m+1}^2 \; t_m^{\alpha-3} \int_{t_{m-\frac{1}{2}}}^{t_{m+\frac{1}{2}}} (t_n - \mathfrak{p})^{-\alpha} d\mathfrak{p} \right\} \\
&\leq C \tau_n^2 \; t_{n-1}^{\alpha-3} \; (t_n - t_{n-\frac{1}{2}})^{1-\alpha} \\
&\leq C \big(T N^{-\gamma} n^{\gamma-1} \big)^2 \; T^{\alpha-3} \left(\frac{n-1}{N} \right)^{\gamma(\alpha-3)} \left(\frac{\tau_n}{2} \right)^{1-\alpha} \\
&\leq C \; n^{-(3-\alpha)}. \qquad (4.27)
\end{aligned}
$$

The bound for $m = 0$ and $m = n-1$ in (4.23) still remains to establish. Suppose $n = 1$ and $m = 0$, then bound for the first term of equation (4.21) becomes

$$
\begin{aligned}
|I_1| &\leq C \int_{t_0}^{t_{\frac{1}{2}}} (t_1 - \mathfrak{p})^{1-\alpha} \; \frac{\partial v(\mathfrak{p})}{\partial \mathfrak{p}} \; d\mathfrak{p} \\
&\leq C \int_{t_0}^{t_{\frac{1}{2}}} (t_1 - \mathfrak{p})^{1-\alpha} \; \mathfrak{p}^{\alpha-2} \; d\mathfrak{p} \\
&\leq C \left[\frac{1}{\alpha - 1} \big(t_1 - t_{\frac{1}{2}} \big)^{1-\alpha} \; t_{\frac{1}{2}}^{\alpha-1} - \frac{1}{\alpha} \; \big(t_1 - t_{\frac{1}{2}} \big)^{-\alpha} \; \mathfrak{p}^{\alpha} \Big|_{t_0}^{t_{\frac{1}{2}}} \right] \\
&\leq C \left(\frac{t_1 - t_{\frac{1}{2}}}{t_{\frac{1}{2}}} \right)^{1-\alpha} \\
&\leq C. \qquad (4.28)
\end{aligned}
$$

Now, considering the second term of (4.21) to show the bound for $n = 1$ and $m = 0$ as:

$$
\begin{aligned}
|I_2| &\leq C \int_{t_0}^{t_{\frac{1}{2}}} (t_1 - \mathfrak{p})^{1-\alpha} \; \frac{2}{\tau_1} \; (v^{\frac{1}{2}} - v^0) \; d\mathfrak{p} \\
&\leq C \; \frac{\big[(t_1 - t_0)^{2-\alpha} - (t_1 - t_{\frac{1}{2}})^{2-\alpha} \big]}{\tau_1} \int_{t_0}^{t_{\frac{1}{2}}} \frac{\partial v(\mathfrak{p})}{\partial \mathfrak{p}} \; d\mathfrak{p} \\
&\leq C \; \frac{\big[(t_1 - t_0)^{2-\alpha} - (t_1 - t_{\frac{1}{2}})^{2-\alpha} \big]}{\tau_1} \int_{t_0}^{t_{\frac{1}{2}}} \mathfrak{p}^{\alpha-2} \; d\mathfrak{p} \\
&\leq C \; \frac{\big[(t_1 - t_0)^{2-\alpha} - (t_1 - t_{\frac{1}{2}})^{2-\alpha} \big]}{\tau_1} \; t_{\frac{1}{2}}^{\alpha-1}
\end{aligned}
$$

$$\leq C\ \tau_1^{2-\alpha}\ \tau_1^{\alpha-2}. \tag{4.29}$$

Now, we consider the case when $n > 1$ and $m = 0$. Then bound for the first term of (4.21)

$$\begin{aligned}
|I_3| &\leq C \int_{t_0}^{t_{\frac{1}{2}}} (t_n - \mathfrak{p})^{1-\alpha}\ \mathfrak{p}^{\alpha-2}\ d\mathfrak{p} \\
&\leq C\left[\frac{1}{\alpha-1}\big(t_n - t_{\frac{1}{2}}\big)^{1-\alpha}\ t_{\frac{1}{2}}^{\alpha-1} - (t_n - t_{\frac{1}{2}})^{-\alpha} \int_{t_0}^{t_{\frac{1}{2}}} \mathfrak{p}^{\alpha-1} d\mathfrak{p}\right] \\
&\leq C\left[\frac{1}{(\alpha-1)}\left(\frac{t_n - t_{\frac{1}{2}}}{t_{\frac{1}{2}}}\right)^{1-\alpha} - \frac{1}{\alpha}\left(\frac{t_n - t_{\frac{1}{2}}}{t_{\frac{1}{2}}}\right)^{-\alpha}\right] \\
&\leq C\left[\frac{t_n - t_{\frac{1}{2}}}{t_{\frac{1}{2}}} + \frac{1}{\alpha} - 1\right]\left(\frac{t_n - t_{\frac{1}{2}}}{t_{\frac{1}{2}}}\right)^{-\alpha} \\
&\leq C\left(\frac{t_n - t_{\frac{1}{2}}}{t_{\frac{1}{2}}}\right)^{1-\alpha} \\
&\leq Cn^{-\gamma(\alpha-1)}.
\end{aligned} \tag{4.30}$$

Here, we establish bound for second term in (4.21) for $n > 1$ and $m = 0$ as follows:

$$\begin{aligned}
|I_4| &\leq C \int_{t_0}^{t_{\frac{1}{2}}} (t_n - \mathfrak{p})^{1-\alpha} \left(\frac{v^{\frac{1}{2}} - v^0}{t_{\frac{1}{2}} - t_0}\right) d\mathfrak{p} \\
&\leq C\ \frac{[t_n^{2-\alpha} - (t_n - t_{\frac{1}{2}})^{2-\alpha}]}{(2-\alpha)}\ \frac{2}{\tau_1} \int_{t_0}^{t_{\frac{1}{2}}} \frac{\partial v(\mathfrak{p})}{\partial \mathfrak{p}}\ d\mathfrak{p} \\
&\leq C\ \frac{[t_n^{2-\alpha} - (t_n - t_{\frac{1}{2}})^{2-\alpha}]}{\tau_1} \int_{t_0}^{t_{\frac{1}{2}}} \mathfrak{p}^{\alpha-2}\ d\mathfrak{p} \\
&\leq C\ [t_n^{2-\alpha} - (t_n - t_{\frac{1}{2}})^{2-\alpha}]\ t_1^{\alpha-2} \\
&\leq C\ \left(\frac{2t_n - t_1}{t_1}\right)^{2-\alpha} \\
&\leq C\ n^{-\gamma(\alpha-1)}.
\end{aligned} \tag{4.31}$$

For $m = n-1$ in equation (4.21), we obtain

$$
\begin{aligned}
&|\varepsilon_1^{(\alpha)}| \\
&\leq C\left|\int_{t_{n-\frac{3}{2}}}^{t_{n-\frac{1}{2}}}(t_n-\mathfrak{p})^{1-\alpha}\left\{\frac{\partial v(\mathfrak{p})}{\partial \mathfrak{p}}-\frac{v^{n-\frac{1}{2}}-v^{n-\frac{3}{2}}}{t_{n-\frac{1}{2}}-t_{n-\frac{3}{2}}}\right\}d\mathfrak{p}\right| \\
&\leq C\left|\max_{\varpi_4,\varpi_5\in(t_{n-\frac{3}{2}},\ t_{n-\frac{1}{2}})}\left(\frac{\partial v(\varpi_4)}{\partial t}-\frac{\partial v(\varpi_5)}{\partial t}\right)\int_{t_{n-\frac{3}{2}}}^{t_{n-\frac{1}{2}}}(t_n-\mathfrak{p})^{1-\alpha}\,d\mathfrak{p}\right| \\
&\leq C\left|(t_{n-\frac{1}{2}}-t_{n-\frac{3}{2}})\max_{\varpi_6\in(t_{n-\frac{3}{2}},\ t_{n-\frac{1}{2}})}\left(\frac{\partial^2 v(\varpi_6)}{\partial t^2}\right)[(t_n-t_{n-\frac{3}{2}})^{2-\alpha}-(t_n-t_{n-\frac{1}{2}})^{2-\alpha}]\right| \\
&\leq C\left|\frac{\tau_n+\tau_{n-1}}{2}\max_{\varpi_6\in(t_{n-\frac{3}{2}},\ t_{n-\frac{1}{2}})}\left(\frac{\partial^3 u(\varpi_6)}{\partial t^3}\right)(t_n-t_{n-\frac{3}{2}})^{2-\alpha}\right| \\
&\leq C\ \tau_n\ (t_{n-\frac{3}{2}})^{\alpha-3}\left(\frac{2t_n-t_{n-1}-t_{n-2}}{2}\right)^{2-\alpha} \\
&\leq C\ \tau_n^{3-\alpha}\left(\frac{t_{n-1}+t_{n-2}}{2}\right)^{\alpha-3} \\
&\leq C\ \tau_n^{3-\alpha}\ t_{n-1}^{\alpha-3} \\
&\leq C\big(TN^{-\gamma}n^{\gamma-1}\big)^{3-\alpha}\left(TN^{-\gamma}(n-1)^{\gamma}\right)^{\alpha-3} \\
&\leq C\ n^{-(3-\alpha)}. \qquad (4.32)
\end{aligned}
$$

Now utilizing inequities (4.10) and (4.24) to get the error bound on $[t_{n-\frac{1}{2}}, t_n]$, we obtain

$$
\begin{aligned}
|\varepsilon_2^{(\alpha)}| &\leq C\frac{(1-\alpha)}{\Gamma(2-\alpha)}(t_n-t_{n-\frac{1}{2}})^2\max_{t\in(t_{n-\frac{1}{2}},\ t_n)}\left|\frac{\partial^2 v(t)}{\partial t^2}\right|\frac{1}{(1-\alpha)}(t_n-t_{n-\frac{1}{2}})^{1-\alpha} \\
&\leq C(t_n-t_{n-\frac{1}{2}})^{3-\alpha}\max_{t\in(t_{n-\frac{1}{2}},\ t_n)}\left|\frac{\partial^3 u(t)}{\partial t^3}\right| \\
&\leq C\left(\frac{\tau_n}{2}\right)^{3-\alpha}t_{n-\frac{1}{2}}^{\alpha-3} \\
&\leq C(TN^{-\gamma}n^{\gamma-1})^{3-\alpha}\left(\frac{n}{N}\right)^{\gamma(\alpha-3)}T^{\alpha-3} \\
&\leq Cn^{-(3-\alpha)}. \qquad (4.33)
\end{aligned}
$$

□

Lemma 4.2.2. Suppose u satisfies the regularity condition defined in (4.10). Then the local consistent error $\widehat{\mathcal{R}}_1^n$ at grid $t = t_n$ holds the following inequality

$$\sum_{n=1}^{k}|\widehat{\mathcal{R}}_1^n| \leq \widetilde{C}_1 + \widetilde{C}_2 \sum_{n=2}^{k} \tau_n^{3-\alpha} t_{n-1}^{\alpha-3}, \quad 1 \leq k \leq N. \tag{4.34}$$

Proof. Form equation (4.15), the bound for $n = 1$ is obtained as,

$$\begin{aligned} |\widehat{\mathcal{R}}_1^n| &\leq \frac{2}{\Gamma(3-\alpha)}\big(\mathcal{C}_{1,0}^{(\alpha)} + \mathcal{S}(1)\big)\mathcal{R}_1^{1/2}, \\ &\leq \frac{2}{\Gamma(3-\alpha)}\tau_1^{1-\alpha}\mathcal{R}_1^{1/2} \\ &\leq \frac{1}{12\Gamma(3-\alpha)}\tau_1^{3-\alpha}t_1^{\alpha-3}. \end{aligned} \tag{4.35}$$

Suppose $\mu = \frac{\Gamma(3-\alpha)}{2}$, then for $n \geq 2$

$$\begin{aligned} &\sum_{n=2}^{k}|\widehat{\mathcal{R}}_1^n| \\ &\leq \frac{1}{\mu}\Big|\sum_{n=2}^{k}\Big[\sum_{m=1}^{n-1}\mathcal{C}_{n,m}^{(\alpha)}\big(\mathcal{R}_1^{m+1/2} - \mathcal{R}_1^{m-1/2}\big) + \mathcal{S}(n)\big(\mathcal{R}_1^{n-1/2} - \mathcal{R}_1^{n-3/2}\big)\Big]\Big|, \\ &\leq \frac{1}{\mu}\Big[\sum_{n=2}^{k}\mathcal{C}_{n,n-1}^{(\alpha)}\mathcal{R}_1^{n-1/2} + \sum_{n=3}^{k}\sum_{m=2}^{n-1}\big(\mathcal{C}_{n,m}^{(\alpha)} - \mathcal{C}_{n,m-1}^{(\alpha)}\big)\mathcal{R}_1^{m-1/2} + 2\sum_{n=2}^{k}\mathcal{S}(n)\mathcal{R}_1^{n-1/2}\Big] \\ &\leq \frac{1}{\mu}\Big[\sum_{n=2}^{k}\mathcal{C}_{n,n-1}^{(\alpha)}\mathcal{R}_1^{n-1/2} + \sum_{m=2}^{k-1}\sum_{n=m+1}^{k}\big(\mathcal{C}_{n,m}^{(\alpha)} - \mathcal{C}_{n,m-1}^{(\alpha)}\big)\mathcal{R}_1^{m-1/2} + 2\sum_{n=2}^{k}\mathcal{S}(n)\mathcal{R}_1^{n-1/2}\Big], \\ &\leq \frac{1}{\mu}\Big[\sum_{n=2}^{k}\mathcal{C}_{n,n-1}^{(\alpha)}\mathcal{R}_1^{n-1/2} + \sum_{m=2}^{k-1}\Big(\mathcal{C}_{m+1,m}^{(\alpha)} - \mathcal{C}_{k,m-1}^{(\alpha)}\Big)\mathcal{R}_1^{m-1/2} + 2\sum_{n=2}^{k}\mathcal{S}(n)\mathcal{R}_1^{n-1/2}\Big], \\ &\leq \frac{1}{\mu}\Big[\sum_{n=2}^{k}\mathcal{C}_{n,n-1}^{(\alpha)}\mathcal{R}_1^{n-1/2} + \sum_{m=2}^{k-1}\mathcal{C}_{m+1,m}^{(\alpha)}\mathcal{R}_1^{m-1/2} + 2\sum_{n=2}^{k}\mathcal{S}(n)\mathcal{R}_1^{n-1/2}\Big], \\ &\leq \frac{2}{\mu}\sum_{n=2}^{k}\big(\mathcal{C}_{n,n-1}^{(\alpha)} + \mathcal{S}(n)\big)\mathcal{R}_1^{n-1/2}, \end{aligned}$$

$$
\begin{aligned}
&\leq \frac{2}{\mu}\frac{1}{2^{2-\alpha}}\sum_{n=2}^{k}\frac{(2\tau_n+\tau_{n-1})^{2-\alpha}}{(\tau_n+\tau_{n-1})}\mathcal{R}_1^{n-1/2},\\
&\leq \frac{2^{\alpha-1}}{\mu}\sum_{n=2}^{k}\frac{\left(2+\frac{\tau_{n-1}}{\tau_n}\right)^{2-\alpha}}{\left(1+\frac{\tau_{n-1}}{\tau_n}\right)}\tau_n^{1-\alpha}\frac{1}{24}\tau_n^2 t_{n-1}^{\alpha-3},\\
&\leq \widetilde{C}_2\sum_{n=2}^{k}\tau_n^{3-\alpha}t_{n-1}^{\alpha-3}. \qquad (4.36)
\end{aligned}
$$

□

4.3 Methodology of the Linearized Difference Scheme

4.3.1 Scheme for One-Dimensional Problem

This section introduces a difference method to estimate the numerical solution of the nonlinear time-fractional diffusion-wave equation (4.1)-(4.3). We divide the spatial range $[0, L]$ into equally spaced node points with spatial step-size $h = \frac{L}{M}$. We consider the uniform space grids domain $\Omega_h = \{x_i \mid x_i = ih; i = 1, ..., M-1\}$ with $\overline{\Omega}_h = \Omega_h \cup \partial\Omega_h$.

To calculate the approximate solution of problem (4.1)-(4.3), we introduce difference scheme on the families $\overline{\Omega}_\tau$ and $\overline{\Omega}_h$ of grid points. Then the considered model (4.1)-(4.3) at node (x_i, t_n) $(1 \leq i \leq M-1,\ 1 \leq n \leq N-1)$ can be written as:

$$
\begin{cases}
{}^{C}\mathcal{D}_{0,t}^{\alpha}u(x_i,t_n) + q(x_i)F\big(u(x_i,t_n)\big) = \frac{\partial}{\partial x}\big(p(x)\frac{\partial u(x,t)}{\partial x}\big)\Big|_{(x_i,t_n)} + f(x_i,t_n) + \mathcal{R}_3,\\
u(x_i,0) = \phi(x_i), \quad u_t(x_i,0) = \varphi(x_i), \quad 1 \leq i \leq M-1,\\
u(x_i,t_n) = \Phi(x_i,t_n), \qquad i \in \{0, M\},\ 1 \leq n \leq N-1.
\end{cases} \qquad (4.37)
$$

Now, we adopt the approximation process for TFCD of order $1 < \alpha < 2$ defined in (4.14).

$$\begin{aligned}\frac{1}{\mu}\Bigg[\sum_{m=0}^{n-1}\mathcal{C}_{n,m}^{(\alpha)}\delta_t {u_i}^{m+\frac{1}{2}} - \sum_{m=1}^{n-1}\mathcal{C}_{n,m}^{(\alpha)}\delta_t {u_i}^{m-\frac{1}{2}} + \mathcal{S}(n)\Big\{\delta_t {u_i}^{n-\frac{1}{2}} - \delta_t {u_i}^{n-\frac{3}{2}}\Big\}\Bigg] + q_i F(u_i^n)\\ = \frac{1}{h^2}\left[\widetilde{p}_{i+1}\ u_{i+1}^n - \left(\widetilde{p}_{i+1}+\widetilde{p}_i\right)\ u_i^n + \widetilde{p}_i\ u_{i-1}^n\right]\\ + f_i^n + \mathcal{R}_1^n + \mathcal{R}_t^{(\alpha)} + (\mathcal{R}_s)_i^n,\ \ (i,j)\in\Omega_h\times\Omega_\tau,\end{aligned} \tag{4.38}$$

where $\mu = \frac{\Gamma(3-\alpha)}{2}$ and

$$\frac{\partial}{\partial x}\left(p(x)\frac{\partial u}{\partial x}\right)\Bigg|_{(x_i,t_n)} = \frac{\widetilde{p}_{i+1}u_{i+1}^n - (\widetilde{p}_{i+1}+\widetilde{p}_i)u_i^n + \widetilde{p}_i u_{i-1}^n}{h^2} + \mathcal{O}(h^2) := \mathcal{H}u_i^n + (\mathcal{R}_s)_i^n, \tag{4.39}$$

$$\frac{\partial^2 u(x,t)}{\partial x^2}\Bigg|_{(x_i,t_n)} = \frac{u_{i+1}^n - 2u_i^n + u_{i-1}^n}{h^2}, \qquad \frac{\partial p(x)}{\partial x}\Bigg|_{x_i} = \frac{p_{i+1}-p_i}{h},\ 1\le i\le M-1,$$

where $\mathcal{H}$ is an approximation of the operator $\frac{\partial}{\partial x}\big(p(x)\frac{\partial}{\partial x}\big)$ and $\widetilde{p}$ approximates p with the replacement $\widetilde{p}_i = p_{i-\frac{1}{2}}$. We use Taylor expansion of $F(u_i^n)$ to obtain the linearized scheme from equation (4.38). Then $F(u_i^1) = F(u_i^0) + (\mathcal{R}_u)_i^1$, for $n = 1$ and

$$\begin{aligned}F(u_i^n) &= F(u_i^{n-1}) + (u_i^n - u_i^{n-1})\partial_u F(u_i^{n-1}) + (\mathcal{R}_u)_i^n\\ &= \widetilde{F}(u_i^{n-1}) + (\mathcal{R}_u)_i^n, \quad 2\le n\le N,\end{aligned} \tag{4.40}$$

where,

$$|(\mathcal{R}_u)_i^1| \le C_4\tau_1^\alpha, \qquad |(\mathcal{R}_u)_i^n| \le C_5\tau_n^2 t_n^{\alpha-2},\ \ \forall\ n\ge 2. \tag{4.41}$$

If $U_{i,j}^n$ is the approximate solution of the problem (4.1), then we get

$$F(U_i^n) - F(u_i^n) = F(U_i^n) - (F(U_i^n) - (\mathcal{R}_u)_i^n)$$

$$= F(U_i^n) - \widetilde{F}(U_i^{n-1}) + (\mathcal{R}_u)_i^n$$
$$= [F(U_i^n) - F(U_i^{n-1})] - (U_i^n - U_i^{n-1})F'(U_i^{n-1}) + (\mathcal{R}_u)_i^n \quad (4.42)$$

where, $(\mathcal{R}_s)_i^n$ and $\mathcal{R}_t^{(\alpha)}$, $\widehat{\mathcal{R}}_1^n$, $(\mathcal{R}_u)_i^n$ denotes the spatial and temporal truncation errors, respectively.

Next, we derive the linearized implicit difference scheme using (4.40) into (4.38)

$$\left[\frac{\mathcal{C}_{n,n-1}^{(\alpha)} + \mathcal{S}(n)}{\tau_n}\right](u_i^n - u_i^{n-1}) - \frac{\mu}{h^2}\left[\widetilde{p}_{i+1}u_{i+1}^n - (\widetilde{p}_{i+1} + \widetilde{p}_i)u_i^n + \widetilde{p}_i u_{i-1}^n\right]$$
$$= \sum_{m=1}^{n-1}\left\{\left(\mathcal{C}_{n,m}^{(\alpha)} - \mathcal{C}_{n,m-1}^{(\alpha)}\right)\delta_t u_i^{m-\frac{1}{2}}\right\} - \mathcal{S}(n)\delta_t u_i^{n-\frac{3}{2}}$$
$$+ \mu f_i^n - \mu q_i \widetilde{F}(u_i^{n-1}) + \mathfrak{R}_i^n, \ (x_i, t_n) \in \Omega_h \times \Omega_\tau, \quad (4.43)$$

$$\left[\frac{-\mu}{h^2}\widetilde{p}_{i+1}\right]u_{i+1}^n + \left[\frac{\mathcal{C}_{n,n-1}^{(\alpha)} + \mathcal{S}(n)}{\tau_n} + \frac{\mu}{h^2}\ (\widetilde{p}_{i+1} + \widetilde{p}_i)\right]u_i^n + \left[\frac{-\mu}{h^2}\widetilde{p}_i\right]u_{i-1}^n$$
$$= \left[\frac{\mathcal{C}_{n,n-1}^{(\alpha)} + \mathcal{S}(n)}{\tau_n}\right]u_i^{n-1} + \sum_{m=1}^{n-1}\left(\mathcal{C}_{n,m}^{(\alpha)} - \mathcal{C}_{n,m-1}^{(\alpha)}\right)\delta_t u_i^{m-\frac{1}{2}}$$
$$+ \mathcal{S}(n)\delta_t u_i^{n-\frac{3}{2}} - \mu q_i \widetilde{F}(u_i^{n-1}) + \mu f_i^n + \mathfrak{R}_i^n, n \geq 1, \quad (4.44)$$

where

$$|\mathfrak{R}_i^n| \leq C(N^{-\min(3-\alpha,\gamma(\alpha-1))} + h^2), \quad (4.45)$$

and C is a positive constant. We substitute the numerical solution U_i^n, for the analytical solution u_i^n in order to eliminate the error term in equation (4.44). Consequently, we obtain the numerical scheme into a brief format:

$$\mathcal{A}U^n = \mathcal{B}, \quad (4.46)$$

where

$$\begin{cases} \mathcal{A}U^n & = \frac{-\mu}{h^2}\widetilde{p}_{i+1}U_{i+1}^n + \left[\frac{\mathcal{C}_{n,n-1}^{(\alpha)}+\mathcal{S}(n)}{\tau_n} + \frac{\mu}{h^2}\ (\widetilde{p}_{i+1}+\widetilde{p}_i)\right]U_i^n + \frac{-\mu}{h^2}\widetilde{p}_i U_{i-1}^n \\ \mathcal{B} & = \left[\frac{\mathcal{C}_{n,n-1}^{(\alpha)}+\mathcal{S}(n)}{\tau_n}\right]U_i^{n-1} + \sum_{m=1}^{n-1}\left(\mathcal{C}_{n,m}^{(\alpha)} - \mathcal{C}_{n,m-1}^{(\alpha)}\right)\delta_t U_i^{m-\frac{1}{2}} \\ & \quad +\mathcal{S}(n)\delta_t U_i^{n-\frac{3}{2}} - \mu q_i \widetilde{F}(U_i^{n-1}) + \mu f_i^n,\ (x_i,t_n)\in\Omega_h\times\Omega_\tau. \end{cases} \tag{4.47}$$

4.3.2 Extension to the Multi-Term Time-Fractional Diffusion-Wave Equation

Here, we consider a generalization of our single-term nonlinear TFDW problem (4.1)-(4.3) to multi-term nonlinear TFDW model which is defined as follows:

$$\sum_{r=0}^{k}\omega_r\ {}^{C}\mathcal{D}_{0,t}^{\alpha_r}u(x,t) = \frac{\partial}{\partial x}\left(p(x)\frac{\partial u}{\partial x}\right) - q(x)F(u) + f(x,t),\ x\in\Omega,\ t\in(0,T], \tag{4.48}$$

where $1<\alpha_k<\alpha_{k-1}<...<\alpha_1<\alpha_0<2$, $\omega_r\geq 0$, $r=0,1,...,k$, $k\in\mathbb{N}$ with the same initial and boundary conditions as mentioned in (4.2)-(4.3). Then the approximate formula of multi-term time-fractional derivatives of order $1<\alpha_r<2$, $0\leq r\leq k$ at grid $t=t_n$ is given as:

$$\begin{aligned} {}^{C}\mathcal{D}_{0,t}^{\alpha_r}u(t_n) =& \frac{1}{\mu_r}\Bigg[\sum_{m=0}^{n-1}\mathcal{C}_{n,m,r}^{(\alpha_r)}\delta_t u^{m+\frac{1}{2}} - \sum_{m=1}^{n-1}\mathcal{C}_{n,m,r}^{(\alpha_r)}\delta_t u^{m-\frac{1}{2}} \\ & + \mathcal{S}(n,r)\left\{\delta_t u^{n-\frac{1}{2}} - \delta_t u^{n-\frac{3}{2}}\right\}\Bigg] + \mathcal{R}_t^{(\alpha_r)} + \widehat{\mathcal{R}}_2^n,\quad n\geq 1, \end{aligned} \tag{4.49}$$

where, the coefficients of equation (4.49) are given as:

$$\mathcal{C}_{n,0,r}^{(\alpha)} = \frac{1}{\tau_1}\left[(t_n-t_0)^{2-\alpha_r} - 2^{\alpha_r-2}(2t_n-t_0-t_1)^{2-\alpha_r}\right],\quad n\geq 1, \tag{4.50}$$

$$\mathcal{C}_{n,m,r}^{(\alpha)} = \frac{(t_n - t_{m-\frac{1}{2}})^{2-\alpha_r} - (t_n - t_{m+\frac{1}{2}})^{2-\alpha_r}}{\tau_m + \tau_{m+1}}, \quad 1 \le m \le n, \tag{4.51}$$

$$\mathcal{S}(n,r) = 2^{\alpha_r - 2} \frac{\tau_n^{2-\alpha_r}}{\tau_n + \tau_{n-1}}, \quad n \ge 1. \tag{4.52}$$

By using equations (4.39), (4.40) and (4.49) into the problem (4.48) at point (x_i, t_n), it yields:

$$\begin{aligned}
&\sum_{r=0}^{k} \left\{ \frac{\omega_r}{\mu_r} \left[\sum_{m=0}^{n-1} \mathcal{C}_{n,m,r}^{(\alpha_r)} \delta_t u_i^{m+\frac{1}{2}} - \sum_{m=1}^{n-1} \mathcal{C}_{n,m,r}^{(\alpha_r)} \delta_t u_i^{m-\frac{1}{2}} + \mathcal{S}(n,r) \left(\delta_t u_i^{n-\frac{1}{2}} - \delta_t u_i^{n-\frac{3}{2}} \right) \right] \right\} \\
&+ q_i F(u_i^n) = \frac{1}{h^2} \left[\widetilde{p}_{i+1}\ u_{i+1}^n - \left(\widetilde{p}_{i+1} + \widetilde{p}_i \right)\ u_i^n + \widetilde{p}_i\ u_{i-1}^n \right] + f_i^n + (\mathcal{R}_t)_i^n + (\mathcal{R}_s)_i^n, \\
&\left[\frac{-\widetilde{p}_{i+1}}{h^2} \right] u_{i+1}^n + \left[\sum_{r=0}^{k} \left\{ \frac{\omega_r}{\mu_r} \left(\frac{\mathcal{C}_{n,n-1,r}^{\alpha_r} + \mathcal{S}(n,r)}{\tau_n} \right) \right\} + \frac{1}{h^2} (\widetilde{p}_{i+1} + \widetilde{p}_i) \right] u_i^n + \left[\frac{-\widetilde{p}_i}{h^2} \right] u_{i-1}^n \\
&= \sum_{r=0}^{k} \left\{ \frac{\omega_r}{\mu_r} \left(\frac{\mathcal{C}_{n,n-1,r}^{\alpha_r} + \mathcal{S}(n,r)}{\tau_n} \right) \right\} u_i^{n-1} + \sum_{r=0}^{k} \left\{ \frac{\omega_r}{\mu_r} \left[\sum_{m=1}^{n-1} \left(\mathcal{C}_{n,m,r}^{(\alpha_r)} - \mathcal{C}_{n,m-1,r}^{(\alpha_r)} \right) \delta_t u_i^{m-\frac{1}{2}} \right] \right\} \\
&+ \sum_{r=0}^{k} \frac{\omega_r}{\mu_r} \mathcal{S}(n,r) \delta_t u_i^{n-\frac{3}{2}} - q_i \widetilde{F}(u_i^{n-1}) + f_i^n + \widehat{\mathfrak{R}}_i^n, \quad (x_i, t_n) \in \Omega_h \times \Omega_\tau.
\end{aligned} \tag{4.53}$$

where

$$|\widehat{\mathfrak{R}}_i^n| \le \widehat{C}(N^{-\min(3-\alpha_r, \gamma(\alpha_r - 1))} + h^2), \tag{4.54}$$

$\widehat{C}$ is a positive constant, $\mu_r = \frac{\Gamma(3-\alpha_r)}{2}$ $(0 \le r \le k)$ and $\widetilde{p}_i = p_{i-\frac{1}{2}}$ as stated in (4.39). The compact form representation of the equation (4.53) with numerical solution U_i^n in place of analytical solution u_i^n, we obtain

$$\begin{aligned}
&\left[\frac{-\widetilde{p}_{i+1}}{h^2} \right] U_{i+1}^n + \left[\sum_{r=0}^{k} \left\{ \frac{\omega_r}{\mu_r} \left(\frac{\mathcal{C}_{n,n-1,r}^{\alpha_r} + \mathcal{S}(n,r)}{\tau_n} \right) \right\} + \frac{1}{h^2} (\widetilde{p}_{i+1} + \widetilde{p}_i) \right] U_i^n + \left[\frac{-\widetilde{p}_i}{h^2} \right] U_{i-1}^n \\
&= \sum_{r=0}^{k} \left\{ \frac{\omega_r}{\mu_r} \left(\frac{\mathcal{C}_{n,n-1,r}^{\alpha_r} + \mathcal{S}(n,r)}{\tau_n} \right) \right\} U_i^{n-1} + \sum_{r=0}^{k} \left\{ \frac{\omega_r}{\mu_r} \left[\sum_{m=1}^{n-1} \left(\mathcal{C}_{n,m,r}^{(\alpha_r)} - \mathcal{C}_{n,m-1,r}^{(\alpha_r)} \right) \right. \right. \\
&\left. \left. \delta_t U_i^{m-\frac{1}{2}} \right] \right\} + \sum_{r=0}^{k} \frac{\omega_r}{\mu_r} \mathcal{S}(n,r) \delta_t U_i^{n-\frac{3}{2}} - q_i \widetilde{F}(U_i^{n-1}) + f_i^n, \quad (x_i, t_n) \in \Omega_h \times \Omega_\tau.
\end{aligned} \tag{4.55}$$

4.3.3 The Two Dimensional Difference Scheme

Suppose h_1 and h_2 denote the step sizes for spatial directions where $h_1 = \frac{L_1}{M_1}$ and $h_2 = \frac{L_2}{M_2}$, and corresponding grid points are $x_i = ih_1$ and $y_j = jh_2$, respectively. The domain of mesh points is $\Omega_s = \{(x_i, y_j)|1 \leq i \leq M_1 - 1,\ 1 \leq j \leq M_2 - 1\}$ with $\overline{\Omega}_s = \Omega \cup \partial\Omega$. Denote the grid function space $\mathfrak{U} = \{u(x_i, y_j, t_n) = u^n_{i,j}|0 \leq i \leq M_1,\ 0 \leq j \leq M_2,\ 0 \leq n \leq N\}$. Consider the evaluation of functions at given grids as $F(u(x_i, y_j, t_n)) = F(u^n_{i,j})$, $f(x_i, y_j, t_n) = f^n_{i,j}$. $(i, j) \in \overline{\Omega}_s$, $n \geq 0$. For any $u \in \mathfrak{U}$, we establish the following notations:

$$\begin{cases} \delta_{\overline{x}} u^n_{i,j} = \frac{u^n_{i,j} - u^n_{i-1,j}}{h_1}, \qquad \delta_x u^n_{i,j} = \frac{u^n_{i+1,j} - u^n_{i,j}}{h_1} \\ \delta_y \delta_{\overline{x}} u^n_{i,j} = \frac{1}{h_1 h_2}[u^n_{i,j+1} - u^n_{i,j} - u^n_{i-1,j+1} + u^n_{i-1,j}] \\ \delta_y \delta_{\overline{x}x} u^n_{i,j} = \frac{1}{h_1^2 h_2}[u^n_{i+1,j+1} - u^n_{i+1,j} - 2u^n_{i,j+1} + 2u^n_{i,j} + u^n_{i-1,j+1} - u^n_{i-1,j}]. \end{cases} \tag{4.56}$$

Similar operators are chosen for variable y. The defined problem (4.1)-(4.3) in two-dimension is as follows:

$$\begin{cases} {}^C\mathcal{D}^{\alpha}_{0,t} u + q(x,y)F(u) = p(\frac{\partial^2 u}{\partial x^2} + \frac{\partial^2 u}{\partial y^2}) + f(x,y,t),\ (x,y,t) \in \Omega \times (0,T], \\ u(x,y,0) = \phi(x,y),\ u_t(x,y,0) = \varphi(x,y),\quad 0 \leq x \leq L_1,\ 0 \leq y \leq L_2, \\ u(x,0,t) = \Psi_1(x,t),\quad u(x,L_2,t) = \Psi_2(x,t),\quad 0 \leq x \leq L_1,\ 0 < t \leq T, \\ u(0,y,t) = \Phi_1(y,t),\quad u(L_1,y,t) = \Phi_2(y,t),\quad 0 \leq y \leq L_2,\ 0 < t \leq T, \end{cases} \tag{4.57}$$

Now, considering the system (4.57) at grid point (x_i, y_j, t_n) and also using the approximation of Caputo derivative in left hand side of (4.57), we get

$$\frac{1}{\mu}\Bigg\{\left[\frac{\mathcal{C}^{(\alpha)}_{n,n-1} + \mathcal{S}(n)}{\tau_n}\right](u^n_{i,j} - u^{n-1}_{i,j}) + \sum_{m=1}^{n-1}\left[\frac{\mathcal{C}^{(\alpha)}_{n,m-1} - \mathcal{C}^{(\alpha)}_{n,m}}{\tau_m}\right](u^m_{i,j} - u^{m-1}_{i,j}) - \frac{\mathcal{S}(n)}{\tau_{n-1}}(u^{n-1}_{i,j} - u^{n-2}_{i,j})\Bigg\} = p\Delta_h u^n_{i,j} - q_{i,j}F(u^n_{i,j}) + f^n_{i,j} + R^n_{i,j},\ (i,j) \in \Omega_s,\ n \geq 1, \tag{4.58}$$

$$u_{i,j}^0 = \phi(x_i, y_j), \quad v_{i,j}^0 = \varphi(x_i, y_j), \quad 1 \le i \le M_1, \ 1 \le j \le M_2, \tag{4.59}$$

$$u_{i,0}^n = \Psi_1(x_i, t_n), \quad u_{i,M_2}^n = \Psi_2(x_i, t_n), \quad 1 \le i \le M_1 - 1, \ 1 \le n \le N, \tag{4.60}$$

$$u_{0,j}^n = \Phi_1(y_j, t_n), \quad u_{M_1,j}^n = \Phi_2(y_j, t_n), \quad 1 \le j \le M_2 - 1, \ 1 \le n \le N, \tag{4.61}$$

where $|R_{i,j}^n| \le C\big(N^{-\min(3-\alpha,\gamma(\alpha-1))} + h_1^2 + h_2^2\big)$ and $\mu = \frac{\Gamma(3-\alpha)}{2}$. Substituting the exact solution $u_{i,j}^n$ with the numerical solution $U_{i,j}^n$ eliminate the error term in equation (4.58), we obtain

$$U_{i,j}^n - \varrho_n \Delta_h U_{i,j}^n = U_{i,j}^{n-1} + \mathcal{I}_n \sum_{m=1}^{n-1} \left[\frac{\mathcal{C}_{n,m}^{(\alpha)} - \mathcal{C}_{n,m-1}^{(\alpha)}}{\tau_m}\right](U_{i,j}^m - U_{i,j}^{m-1}) + \mathcal{I}_n \frac{\mathcal{S}(n)}{\tau_{n-1}}(U_{i,j}^{n-1}$$
$$- U_{i,j}^{n-2}) - \mu \mathcal{I}_n q_{i,j} \widetilde{F}(U_{i,j}^{n-1}) + \mu \mathcal{I}_n f_{i,j}^n, \ (i,j) \in \Omega_s, \quad 1 \le n \le N, \tag{4.62}$$

where, $\mathcal{I}_n = \frac{\tau_n}{\mathcal{C}_{n,n-1}^{(\alpha)} + \mathcal{S}(n)}$ and $\varrho_n = p\mu\mathcal{I}_n$. To develop the ADI scheme, a small term ${}_0\mathcal{D}_t^\alpha \varrho_n^2 \delta_x^2 \delta_y^2 U_{i,j}^n$ is added to equation (4.62), then we obtain

$$(I - \varrho_n \delta_x^2)(I - \varrho_n \delta_y^2) U_{i,j}^n = \big(U_{i,j}^{n-1} + \varrho_n^2 \delta_x^2 \delta_y^2 U_{i,j}^{n-1}\big) + \mathcal{I}_n \frac{\mathcal{S}(n)}{\tau_{n-1}} \big(U_{i,j}^{n-1} + \varrho_n^2 \delta_x^2 \delta_y^2 U_{i,j}^{n-1}$$
$$- U_{i,j}^{n-2} - \varrho_n^2 \delta_x^2 \delta_y^2 U_{i,j}^{n-2}\big) + \mathcal{I}_n \sum_{m=1}^{n-1} \left[\frac{\mathcal{C}_{n,m}^{(\alpha)} - \mathcal{C}_{n,m-1}^{(\alpha)}}{\tau_m}\right] \big(U_{i,j}^m + \varrho_n^2 \delta_x^2 \delta_y^2 U_{i,j}^m - U_{i,j}^{m-1}$$
$$- \varrho_n^2 \delta_x^2 \delta_y^2 U_{i,j}^{m-1}\big) - \mu \mathcal{I}_n q_{i,j} \widetilde{F}(U_{,j}^{n-1}) + \mu \mathcal{I}_n f_{i,j}^n, \ (i,j) \in \Omega_s, \ n \ge 1. \tag{4.63}$$

Suppose intermediate solution $Y_{i,j}^* = (I - \varrho_n \delta_y^2) U_{i,j}^n$, $1 \le i \le M_1 - 1$, $1 \le j \le M_2 - 1$. Initially, we solve the system of equations to determine the intermediate function

$Y^*_{i,j}$, where j is fixed within the range $\{1, 2, ..., M_2 - 1\}$,

$$\begin{cases} (I - \varrho_n\delta_x^2)Y^*_{i,j} = \big(U^{n-1}_{i,j} + \varrho_n^2\delta_x^2\delta_y^2 U^{n-1}_{i,j}\big) + \mathcal{I}_n \frac{\mathcal{S}(n)}{\tau_{n-1}}\big(U^{n-1}_{i,j} + \varrho_n^2\delta_x^2\delta_y^2 U^{n-1}_{i,j} \\ -U^{n-2}_{i,j} - \varrho_n^2\delta_x^2\delta_y^2 U^{n-2}_{i,j}\big) + \mathcal{I}_n \sum_{m=1}^{n-1}\left[\frac{\mathcal{C}^{(\alpha)}_{n,m} - \mathcal{C}^{(\alpha)}_{n,m-1}}{\tau_m}\right]\big(U^m_{i,j} + \varrho_n^2\delta_x^2\delta_y^2 U^m_{i,j} - U^{m-1}_{i,j} \\ -\varrho_n^2\delta_x^2\delta_y^2 U^{m-1}_{i,j}\big) - \mu\mathcal{I}_n q_{i,j}\widetilde{F}(U^{n-1}_{,j}) + \mu\mathcal{I}_n f^n_{i,j},\ 1 \le i \le M_1 - 1,\ n \ge 1. \\ Y^*_{0,j} = (I - \varrho_n\delta_y^2)U^n_{0,j},\ Y^*_{M_1,j} = (I - \varrho_n\delta_y^2)U^n_{M_1,j}. \end{cases} \tag{4.64}$$

Then the final solution $U^n_{i,j}$ can be obtained from the following system, for fix $i \in \{1, 2, ..., M_1 - 1\}$

$$(I - \varrho_n\delta_y^2)U^n_{i,j} = Y^*_{i,j},\quad 1 \le j \le M_2 - 1, \tag{4.65}$$

$$U^n_{i,0} = \Psi_1(x_i, t_n),\quad U^n_{i,M_2} = \Psi_2(x_i, t_n). \tag{4.66}$$

4.4 Stability Analysis

Suppose that $\max\limits_{0\le i\le M}|u^n_i| = |u^n_{i_0}| := \|u^n\|_\infty$, $\max\limits_{0\le i\le M}|p_i| = \|p\|_\infty$, and $\max\limits_{0\le i\le M}|q_i| = \|q\|_\infty$, then the equation (4.1) at the grid point (x_{i_0}, t_n)

$$\Upsilon_1(U^1_{i_0} - U^0_{i_0}) + q_{i_0}\widetilde{F}(U^1_{i_0}) = \frac{\big[\widetilde{p}_{i_0+1}U^1_{i_0+1} - (\widetilde{p}_{i_0+1} + \widetilde{p}_{i_0})U^1_{i_0} + \widetilde{p}_{i_0}U^1_{i_0-1}\big]}{h^2} + f^1_{i_0},\ n = 1, \tag{4.67}$$

$$\begin{aligned}\Upsilon_n(U^n_{i_0} - U^{n-1}_{i_0}) + q_{i_0}\widetilde{F}(U^{n-1}_{i_0}) &= \frac{1}{h^2}\big[\widetilde{p}_{i_0+1}U^n_{i_0+1} - (\widetilde{p}_{i_0+1} + \widetilde{p}_{i_0})U^n_{i_0} + \widetilde{p}_{i_0}U^n_{i_0-1}\big] \\ + \frac{\mathcal{S}(n)}{\tau_{n-1}}(U^{n-1}_{i_0} - U^{n-2}_{i_0}) &+ \sum_{m=1}^{n-1}\left[\frac{\mathcal{C}^{(\alpha)}_{n,m} - \mathcal{C}^{(\alpha)}_{n,m-1}}{\tau_m}\right](U^m_{i_0} - U^{m-1}_{i_0}) + f^n_{i_0},\quad n \ge 2,\end{aligned} \tag{4.68}$$

where $\Upsilon_1 = \frac{\mathcal{C}^{(\alpha)}_{n,0} + \mathcal{S}(1)}{\mu\tau_1} \ge 0$ and $\Upsilon_n = \frac{\mathcal{C}^{(\alpha)}_{n,n-1} + \mathcal{S}(n)}{\mu\tau_n} \ge 0,\ n \ge 2.$

Lemma 4.4.1. The solution U_i^n holds the following bound

$$\|U^1\|_\infty \leq (1+\varkappa_1)\|U^0\|_\infty + \frac{1}{\Upsilon_1}\|f^1\|_\infty, \qquad n=1, \tag{4.69}$$

$$\|U^n\|_\infty \leq (1+\varkappa_2)\|U^{n-1}\|_\infty + \frac{1}{\Upsilon_n}\left|\frac{\mathcal{S}(n)}{\tau_{n-1}}(U_{i_0}^{n-1}-U_{i_0}^{n-2}) + \sum_{m=1}^{n-1}\left[\frac{\mathcal{C}_{n,m}^{(\alpha)}-\mathcal{C}_{n,m-1}^{(\alpha)}}{\tau_m}\right](U_{i_0}^m-U_{i_0}^{m-1})\right| + \frac{1}{\Upsilon_n}\|f^n\|, \quad n\geq 2, \tag{4.70}$$

where $\varkappa_1 = \frac{\|q\|_\infty \mathcal{L}}{\Upsilon_1}$ and $\varkappa_2 = \frac{\|q\|_\infty \mathcal{L}}{\Upsilon_n}$, $n \geq 2$.

Proof. From equations (4.67) and (4.68), we obtain

$$\left[\Upsilon_1 + \frac{1}{h^2}(\widetilde{p}_{i_0+1}+\widetilde{p}_{i_0})\right]U_{i_0}^1 = \Upsilon_1 U_{i_0}^0 + \frac{1}{h^2}\widetilde{p}_{i_0+1}U_{i_0+1}^1 + \frac{1}{h^2}\widetilde{p}_{i_0}U_{i_0-1}^1 - q_{i_0}\widetilde{F}(U_{i_0}^0) + f_{i_0}^1, \tag{4.71}$$

$$\left[\Upsilon_n + \frac{1}{h^2}(\widetilde{p}_{i_0+1}+\widetilde{p}_{i_0})\right]U_{i_0}^n = \Upsilon_n U_{i_0}^{n-1} + \frac{1}{h^2}\widetilde{p}_{i_0+1}U_{i_0+1}^n + \frac{1}{h^2}\widetilde{p}_{i_0}U_{i_0-1}^n + \frac{\mathcal{S}(n)}{\tau_{n-1}}(U_{i_0}^{n-1}-U_{i_0}^{n-2}) + \sum_{m=1}^{n-1}\left[\frac{\mathcal{C}_{n,m}^{(\alpha)}-\mathcal{C}_{n,m-1}^{(\alpha)}}{\tau_m}\right](U_{i_0}^m-U_{i_0}^{m-1}) - q_{i_0}\widetilde{F}(U_{i_0}^{n-1}) + f_{i_0}^n, \quad n\geq 2. \tag{4.72}$$

For the choice of i_0. Equations (4.71) and (4.72) convert into the following inequalities

$$\Upsilon_1\|U^1\|_\infty + \frac{2}{h^2}\|p\|_\infty\|U^1\|_\infty \leq \Upsilon_1\|U^0\|_\infty + \frac{2}{h^2}\|p\|_\infty\|U^1\|_\infty + \|q\|_\infty\mathcal{L}\|U^0\|_\infty + \|f^1\|_\infty, \tag{4.73}$$

$$\Upsilon_n\|U^n\|_\infty + \frac{2}{h^2}\|p\|_\infty\|U^n\|_\infty \leq \Upsilon_n\|U^{n-1}\|_\infty + \frac{2}{h^2}\|p\|_\infty\|U^n\|_\infty + \|q\|_\infty\mathcal{L}\|U^{n-1}\|_\infty + \left|\frac{\mathcal{S}(n)}{\tau_{n-1}}\left(U_{i_0}^{n-1}-U_{i_0}^{n-2}\right) + \sum_{m=1}^{n-1}\left[\frac{\mathcal{C}_{n,m}^{(\alpha)}-\mathcal{C}_{n,m-1}^{(\alpha)}}{\tau_m}\right]\left(U_{i_0}^m-U_{i_0}^{m-1}\right)\right| + \|f^n\|_\infty, \quad n\geq 2. \tag{4.74}$$

These equations (4.73) and (4.74) are equivalent to

$$\|U^1\|_\infty \leq \left(1+\frac{\|q\|_\infty \mathcal{L}}{\Upsilon_1}\right)\|U^0\|_\infty + \frac{1}{\Upsilon_1}\|f^1\|_\infty, \quad n=1, \tag{4.75}$$

$$\begin{aligned}\|U^n\|_\infty \leq \left(1+\frac{\|q\|_\infty \mathcal{L}}{\Upsilon_n}\right)\|U^{n-1}\|_\infty + \frac{1}{\Upsilon_n}\Bigg|\frac{\mathcal{S}(n)}{\tau_{n-1}}\left(U_{i_0}^{n-1}-U_{i_0}^{n-2}\right) \\ + \sum_{m=1}^{n-1}\left[\frac{\mathcal{C}_{n,m}^{(\alpha)}-\mathcal{C}_{n,m-1}^{(\alpha)}}{\tau_m}\right]\left(U_{i_0}^{m}-U_{i_0}^{m-1}\right)\Bigg| + \frac{1}{\Upsilon_n}\|f^n\|_\infty, \quad n\geq 2.\end{aligned} \tag{4.76}$$

□

Now, we show the stability of the scheme (4.44). The equation (4.43) can also be represented as:

$$\begin{aligned}&\left[\frac{\mathcal{C}_{n,n-1}^{(\alpha)}+\mathcal{S}(n)}{\mu\tau_n}\right](u_i^n-u_i^{n-1}) - \frac{1}{h^2}\left[\widetilde{p}_{i+1}u_{i+1}^n-(\widetilde{p}_{i+1}+\widetilde{p}_i)u_i^n+\widetilde{p}_i u_{i-1}^n\right] \\ &\quad = \frac{\mathcal{S}(n)}{\mu\tau_{n-1}}(u_i^{n-1}-u_i^{n-2}) + \sum_{m=1}^{n-1}\left[\frac{\mathcal{C}_{n,m}^{(\alpha)}-\mathcal{C}_{n,m-1}^{(\alpha)}}{\mu\tau_m}\right](u_i^m-u_i^{m-1}) \\ &\quad - q_i\widetilde{F}(u_i^{n-1})+\mu f_i^n+\mathfrak{R}_i^n, \ (x_i,t_n)\in\Omega_h\times\Omega_\tau\end{aligned} \tag{4.77}$$

$$u(x_i,0)=\phi(x_i), \quad u_t(x_i,0)=\varphi(x_i), \quad x_i\in\Omega_h,$$

$$u(x_i,t_n)=\Phi(x_i,t_n), \quad x_i\in\partial\overline{\Omega}_h, \quad t_n\in\Omega_\tau.$$

Suppose the error $\epsilon_i^n = U_i^n - u_i^n$, then we obtain

$$\left[\frac{\mathcal{C}_{n,n-1}^{(\alpha)}+\mathcal{S}(n)}{\mu\tau_n}\right]\zeta_i^n - \frac{1}{h^2}\left[\widetilde{p}_{i+1}\zeta_{i+1}^n-(\widetilde{p}_{i+1}+\widetilde{p}_i)\zeta_i^n+\widetilde{p}_i\zeta_{i-1}^n\right] = \left[\frac{\mathcal{C}_{n,n-1}^{(\alpha)}+\mathcal{S}(n)}{\mu\tau_n}\right]\zeta_i^{n-1}+$$
$$\left[\frac{\mathcal{S}(n)}{\mu\tau_{n-1}}\right](\zeta_i^{n-1}-\zeta_i^{n-2}) + \sum_{m=1}^{n-1}\left[\frac{\mathcal{C}_{n,m}^{(\alpha)}-\mathcal{C}_{n,m-1}^{(\alpha)}}{\mu\tau_m}\right](\zeta_i^m-\zeta_i^{m-1}) - \mathcal{L}q_i\zeta_i^{n-1}, \ 1\leq i\leq M-1,$$
$$\left[-\frac{\widetilde{p}_{i+1}}{h^2}\right]\zeta_{i+1}^n + \left[\frac{\mathcal{C}_{n,n-1}^{(\alpha)}+\mathcal{S}(n)}{\mu\tau_n}+\frac{\widetilde{p}_{i+1}+\widetilde{p}_i}{h^2}\right]\zeta_i^n + \left[-\frac{\widetilde{p}_i}{h^2}\right]\zeta_{i-1}^n = \left[\frac{\mathcal{C}_{n,n-1}^{(\alpha)}+\mathcal{S}(n)}{\mu\tau_n}\right]\zeta_i^{n-1}+$$

$$\left[\frac{\mathcal{S}(n)}{\mu\tau_{n-1}}\right](\zeta_i^{n-1}-\zeta_i^{n-2})+\sum_{m=1}^{n-1}\left[\frac{\mathcal{C}_{n,m}^{(\alpha)}-\mathcal{C}_{n,m-1}^{(\alpha)}}{\mu\tau_m}\right](\zeta_i^{m}-\zeta_i^{m-1})-\mathcal{L}q_i\zeta_i^{n-1},\ n\geq 1. \tag{4.78}$$

For $n \geq 1$, we form the grid function $\zeta(x)$ in the following way

$$\zeta^n(x)=\begin{cases}\zeta_i^n & x_{i-\frac{1}{2}}<x\leq x_{i+\frac{1}{2}},\ 1\leq i\leq M-1,\\ 0, & 0\leq x<\frac{h}{2},\ L-\frac{h}{2}<x\leq L.\end{cases} \tag{4.79}$$

The Fourier series expression for the function $\zeta^n(x)$ is presented as follows:

$$\zeta^n(x)=\sum_{l=-\infty}^{\infty}\rho^n(l)\exp(2\pi\iota lx/L),\quad n\geq 1, \tag{4.80}$$

where the corresponding coefficients $\rho^n(l)$ are referred as:

$$\rho^n(l)=\frac{1}{L}\int_0^L\zeta^n(x)\exp(-2\pi\iota lx/L)ds, \tag{4.81}$$

Consider the solution of equation (4.78) be $\zeta_i^n=\rho^n\exp(\iota(i\sigma h))$, where $\sigma=2\pi l/L$ and $\iota=\sqrt{-1}$. Now, taking the assumed solution into equation (4.78), we obtain

$$\begin{aligned}&\left\{\left[\frac{-\widetilde{p}_{i+1}}{h^2}\right]\exp(\iota\sigma h)+\left[\frac{\mathcal{C}_{n,n-1}^{(\alpha)}+\mathcal{S}(n)}{\mu\tau_n}+\frac{\widetilde{p}_{i+1}+\widetilde{p}_i}{h^2}\right]+\left[\frac{-\widetilde{p}_i}{h^2}\right]\exp(-\iota\sigma h)\right\}\rho^n=\\&\left[\frac{\mathcal{C}_{n,n-1}^{(\alpha)}+\mathcal{S}(n)}{\mu\tau_n}-\mathcal{L}q_i\right]\rho^{n-1}+\frac{\mathcal{S}(n)}{\mu\tau_{n-1}}(\rho^{n-1}-\rho^{n-2})+\sum_{m=1}^{n-1}\left[\frac{\mathcal{C}_{n,m}^{(\alpha)}-\mathcal{C}_{n,m-1}^{(\alpha)}}{\mu\tau_m}\right](\rho^m\\&-\rho^{m-1}),\left[\widehat{\lambda}_1\cos(\sigma h)+\iota\widehat{\lambda}_2\sin(\sigma h)+(\widehat{\lambda}_1+\widehat{\lambda}_3)\right]\rho^n=\left[\widehat{\lambda}_3-\mathcal{L}q_i\right]\rho^{n-1}+\frac{\mathcal{S}(n)}{\mu\tau_{n-1}}(\rho^{n-1}\\&-\rho^{n-2})+\sum_{m=1}^{n-1}\left[\frac{\mathcal{C}_{n,m}^{(\alpha)}-\mathcal{C}_{n,m-1}^{(\alpha)}}{\mu\tau_m}\right](\rho^m-\rho^{m-1}),\ 1\leq i\leq M-1,\ 1\leq n\leq N-1,\end{aligned} \tag{4.82}$$

where $\widehat{\lambda}_1 = \frac{-(\widetilde{p}_{i+1}+\widetilde{p}_i)}{h^2}$, $\widehat{\lambda}_2 = \frac{-(\widetilde{p}_{i+1}-\widetilde{p}_i)}{h^2}$, $\widehat{\lambda}_3 = \frac{\mathcal{C}^{(\alpha)}_{n,n-1}+\mathcal{S}(n)}{\mu\tau_n}$. Rewriting equation (4.82) as:

$$\rho^n = \frac{\big[\widehat{\lambda}_3 - \mathcal{L}q_i\big]\rho^{n-1} + \frac{\mathcal{S}(n)}{\mu\tau_{n-1}}(\rho^{n-1}-\rho^{n-2}) + \sum\limits_{m=1}^{n-1}\left[\frac{\mathcal{C}^{(\alpha)}_{n,m}-\mathcal{C}^{(\alpha)}_{n,m-1}}{\mu\tau_m}\right](\rho^m-\rho^{m-1})}{\big[\widehat{\lambda}_1(1+\cos(\sigma h)) + \iota\widehat{\lambda}_2\sin(\sigma h) + \widehat{\lambda}_3\big]} \tag{4.83}$$

Since $0 < c_1 \le p_i \le c_2$, $q_i \ge 0$, $\forall\ x_i \in \overline{\Omega}_h$, $\tau_{n-1} \le \tau_n$, $n \ge 1$, then the properties for the assumed notations

$$\begin{aligned} 0 < |\widehat{\lambda}_1| \le C_1, \quad 0 < |\widehat{\lambda}_2| \le C_2, \\ \frac{\mathcal{C}^{(\alpha)}_{n,n-1}+\mathcal{S}(n)}{\mu\tau_n} &= \frac{(t_n - t_{n-\frac{3}{2}})^{2-\alpha} - (t_n - t_{n-\frac{1}{2}})^{2-\alpha}}{\mu\tau_n(\tau_n+\tau_{n-1})} + 2^{\alpha-2}\frac{\tau_n^{1-\alpha}}{\mu(\tau_n+\tau_{n-1})}, \\ &= \frac{2^{\alpha-2}}{\mu}\frac{(2\tau_n+\tau_{n-1})^{2-\alpha}}{\tau_n(\tau_n+\tau_{n-1})} > 0, \forall\ n \ge 1, \end{aligned} \tag{4.84}$$

$$|\widehat{\lambda}_1(1+\cos(\sigma h)) + \iota\widehat{\lambda}_2\sin(\sigma h) + \widehat{\lambda}_3| \ge |\widehat{\lambda}_3|,\ n \ge 1. \tag{4.85}$$

Then the equation (4.83) will convert into the following inequality

$$|\rho^n| \le \frac{\left|\widehat{\lambda}_3\rho^{n-1} + \frac{\mathcal{S}(n)}{\mu\tau_{n-1}}(\rho^{n-1}-\rho^{n-2}) + \sum\limits_{m=1}^{n-1}\left[\frac{\mathcal{C}^{(\alpha)}_{n,m}-\mathcal{C}^{(\alpha)}_{n,m-1}}{\mu\tau_m}\right](\rho^m-\rho^{m-1})\right|}{\left|\big[\widehat{\lambda}_1(1+\cos(\sigma h)) + \iota\widehat{\lambda}_2\sin(\sigma h) + \widehat{\lambda}_3\big]\right|},\ n \ge 1. \tag{4.86}$$

Theorem 4.4.1. Let ζ^n $(1 \le n \le N)$ represents the solutions of equation (4.86), then

$$|\zeta^n| \le |\zeta^0|, \quad n \ge 1. \tag{4.87}$$

Proof. Using mathematical induction, we establish the validity of this theorem. For $n = 1$, utilizing equations (4.67) and (4.85), the inequality (4.86) becomes

$$|\rho^1| \leq \frac{\left|\left(\frac{\mathcal{C}_{1,0}^{(\alpha)}+\mathcal{S}(1)}{\mu\tau_1}\right)\rho^0\right|}{\left|\left[\widehat{\lambda}_1(1+\cos(\sigma h)) + \iota\widehat{\lambda}_2\sin(\sigma h) + \left(\frac{\mathcal{C}_{1,0}^{(\alpha)}+\mathcal{S}(1)}{\mu\tau_1}\right)\right]\right|} \leq |\rho^0|. \tag{4.88}$$

Therefore the inequality holds for $n = 1$. Now, we show the bound for $n = 2$ by using (4.88),

$$\begin{aligned}
|\rho^2| &\leq \frac{\left|\left[\frac{\mathcal{C}_{2,1}^{(\alpha)}+\mathcal{S}(2)}{\mu\tau_2} + \frac{\mathcal{C}_{2,1}^{(\alpha)}+\mathcal{S}(2)}{\mu\tau_1} - \frac{\mathcal{C}_{2,0}^{(\alpha)}}{\mu\tau_1}\right]\rho^1 + \left[\frac{\mathcal{C}_{2,0}^{(\alpha)}}{\mu\tau_1} - \frac{\mathcal{C}_{2,1}^{(\alpha)}+\mathcal{S}(2)}{\mu\tau_1}\right]\rho^0\right|}{\left|\left[\widehat{\lambda}_1(1+\cos(\sigma h)) + \iota\widehat{\lambda}_2\sin(\sigma h) + \left(\frac{\mathcal{C}_{2,1}^{(\alpha)}+\mathcal{S}(2)}{\mu\tau_2}\right)\right]\right|}\Bigg|, \\
&\leq \frac{\left|\left[\frac{\mathcal{C}_{2,1}^{(\alpha)}+\mathcal{S}(2)}{\mu\tau_2} + \frac{\mathcal{C}_{2,1}^{(\alpha)}+\mathcal{S}(2)}{\mu\tau_1} - \frac{\mathcal{C}_{2,0}^{(\alpha)}}{\mu\tau_1} + \frac{\mathcal{C}_{2,0}^{(\alpha)}}{\mu\tau_1} - \frac{\mathcal{C}_{2,1}^{(\alpha)}+\mathcal{S}(2)}{\mu\tau_1}\right]\rho^0\right|}{\left|\left[\widehat{\lambda}_1(1+\cos(\sigma h)) + \iota\widehat{\lambda}_2\sin(\sigma h) + \left(\frac{\mathcal{C}_{2,1}^{(\alpha)}+\mathcal{S}(2)}{\mu\tau_2}\right)\right]\right|} \leq |\rho^0|.
\end{aligned} \tag{4.89}$$

Now, assuming that the validity of (4.86) for $n = 1, 2, ..., r-1$, i.e. $|\rho^n| \leq |\rho^0|$ for $1 \leq n \leq r-1$. Let $d_{n,m}^{(\alpha)} = \frac{\mathcal{C}_{n,m}^{(\alpha)} - \mathcal{C}_{n,m-1}^{(\alpha)}}{\mu\tau_m}$, then equation (4.86) yields

$$\begin{aligned}
&|\rho^r| \\
&\leq \left|\frac{\widehat{\lambda}_3\rho^{r-1} + \frac{\mathcal{S}(r)}{\mu\tau_{r-1}}(\rho^{r-1}-\rho^{r-2}) + \sum_{m=2}^{r-1}\left(d_{r,m-1}^{(\alpha)} - d_{r,m}^{(\alpha)}\right)\rho^{m-1} + d_{r,r-1}^{(\alpha)}\rho^{r-1} - d_{r,1}^{(\alpha)}\rho^0}{\left[\widehat{\lambda}_1(1+\cos(\sigma h)) + \iota\widehat{\lambda}_2\sin(\sigma h) + \widehat{\lambda}_3\right]}\right|, \\
&\leq \left|\frac{\widehat{\lambda}_3 + \sum_{m=2}^{r-1}\left(d_{r,m-1}^{(\alpha)} - d_{r,m}^{(\alpha)}\right) + d_{r,r-1}^{(\alpha)} - d_{r,1}^{(\alpha)}}{\left[\widehat{\lambda}_1(1+\cos(\sigma h)) + \iota\widehat{\lambda}_2\sin(\sigma h) + \widehat{\lambda}_3\right]}\right||\rho^0|.
\end{aligned} \tag{4.90}$$

Considering the property of coefficients given in (4.19) and (4.85) into equation (4.86), we obtain

$$|\rho^r| \leq |\rho^0|. \tag{4.91}$$

Hence, according to the principle of induction, (4.86) holds true for all values of n. □

4.5 Numerical Examples

In order to exhibit the accuracy and efficiency of the proposed computational schemes (4.44), (4.55) and (4.64)-(4.66), we consider four numerical examples of the governed problem (4.1)-(4.3) in both one and two-dimensions. In first Example 4.5.1, we considered the three cases including smooth and nonsmooth exact solutions, as well as nonsmooth initial data corresponding to the given problem (4.1)-(4.3). In second problem 4.5.2, we handled nonsmooth solution of the nonlinear time-fractional Telegraph equation with variable coefficients. We explored the numerical solution of the multi-term time-fractional nonlinear diffusion-wave equation with variable coefficients in Example 4.5.3. Example 4.5.4 displays the two-dimensional model corresponding to the problem (4.1)-(4.3) with smooth and nonsmooth exact solutions. We utilize three cases of the function $F(u)$ for the nonlinear term in equation (4.1).

Case 1 $F(u(x,t)) = u^3 - u$, **Case 2** $F(u(x,t)) = \sin(u)$, **Case 3** $F(u(x,t)) = u$.

We employ the subsequent formulas to estimate the error and measure the rate of convergence when the exact solution is known.

$$\mathcal{E}_1(h,\tau) = \max_{1\le i\le M-1} ||u_i^N - U_i^N||_{L_\infty},\ \mathrm{OC}_t = \log_2\left[\frac{\mathcal{E}_1(h,2\tau)}{\mathcal{E}_1(h,\tau)}\right],\ \mathrm{OC}_s = \log_2\left[\frac{\mathcal{E}_1(2h,\tau)}{\mathcal{E}_1(h,\tau)}\right]. \tag{4.92}$$

Example 4.5.1. Consider the following Klein-Gorden and Sine-Gorden TFDW equation (4.1) with variable coefficients

$$ {}^{C}\mathcal{D}^{\alpha}_{0,t}u(x,t) + q(x)F(u(x,t)) = \frac{\partial}{\partial x}\left(p(x)\frac{\partial u(x,t)}{\partial x}\right) + f(x,t), \quad (x,t) \in \Omega \times [0,1], \tag{4.93} $$

Here, we examine the accuracy of scheme (4.44) for the following three cases involving smooth, nonsmooth exact solution and considering discontinuous initial condition.

Case (i) The exact solution of (4.1) is $u(x,t) = t^{\delta}\sin(x),\ x \in [0,\pi],\ t \in (0,1]$. Next the corresponding initial, boundary conditions and force term are defined as:

$$ \begin{cases} u(x,0) = u_t(x,0) = 0, \quad x \in [0,\pi], \\ u(0,t) = u(\pi,t) = 0, \quad t \in (0,1], \\ f(x,t) = \frac{\Gamma(\delta+1)}{\Gamma(\delta+1-\alpha)}t^{\delta-\alpha}\sin(x) - t^{\delta}p'(x)\cos(x) + t^{\delta}p(x)\sin(x) + q(x)F(u(x,t)). \end{cases} \tag{4.94} $$

Case (ii) Consider the nonsmooth exact solution of problem (4.1) as $u(x,t) = (\sqrt[3]{t} + t^{\alpha})\sin(x),\ x \in [0,\pi],\ t \in (0,1]$. The initial, boundary conditions and force term are given as:

$$ \begin{cases} u(x,0) = u_t(x,0) = 0, \quad x \in [0,\pi], \\ u(0,t) = u(\pi,t) = 0, \quad t \in (0,1], \\ f(x,t) = \left(\Gamma(1+\alpha) + \frac{\Gamma(5/2)}{\Gamma(5/2-\alpha)}t^{3/2-\alpha}\right)\sin(x) + (p(x)\sin(x) \\ \qquad\qquad -p'(x)\cos(x) + q(x)\sin(x))(t^{3/2} + t^{\alpha}). \end{cases} \tag{4.95} $$

Case (iii) In this case, we examine the rate of convergence in temporal direction for the homogeneous problem (4.1) with discontinuous initial condition

$$\begin{cases} u(x,0) = \chi_{(0,1/2]}(x), \quad u_t(x,0) = 0, \quad x \in [0,1] \\ u(0,t) = u(1,t) = 0, \quad t \in (0,1], \\ f(x,t) = 0, \end{cases} \tag{4.96}$$

where characteristic function is:

$$\chi_{(0,1/2]}(x) = \begin{cases} 1, & 0 < x \leq 1/2, \\ 0, & \text{elsewhere.} \end{cases}$$

In **Case (iii)**, the exact solution of problem (4.93) is unknown. Then we use the following formula to calculate the accuracy of the scheme (4.44).

$$\mathrm{OC}_t = \log_2 \left(\frac{\left|\left|(U_N^{\tau} - U_N^{\tau/2})\right|\right|_{L_\infty}}{\left|\left|(U_N^{\tau/2} - U_N^{\tau/4})\right|\right|_{L_\infty}} \right).$$

In Tables 4.1-4.5, we display the numerical results in both time and space directions for the **Case (i)** of Example 4.5.1 using scheme (4.44). Tables 4.6 and 4.7 represent the computational results for the **Case (ii)** of Example 4.5.1 through the utilization of the scheme (4.44). Table 4.8 expresses that the defined scheme (4.44) has convergence rate $N^{-(3-\alpha)}$, $1 < \alpha < 2$ for the nonsmooth initial data given in **Case (iii)** of Example 4.5.1. In Table 4.1, we demonstrate the errors and OC in time direction for sufficiently smooth exact solution with $F(u) = u^3 - u$ and two different choices of variable coefficient $p(x)$. One can note that the scheme (4.44) is $(3-\alpha)$ order accurate in time and OC is almost approachable to the expected order of convergence (EOC).

TABLE 4.1: Temporal direction computational errors and convergence order for **Case (i)** of Example 4.5.1 with $\delta = (2+\alpha)$, $q(x) = 1$, $F(u) = u^3 - u$, $M = 2000$ and different choices of coefficient $p(x)$.

		$\alpha = 1.2$		$\alpha = 1.5$		$\alpha = 1.8$	
τ	$p(x)$	$\|u^\tau - U^\tau\|_\infty$	OC	$\|u^\tau - U^\tau\|_\infty$	OC	$\|u^\tau - U^\tau\|_\infty$	OC
1/16	$2 - \sin(3x)$	2.0249E-02		5.0997E-02		1.3335E-01	
1/32		6.2767E-03	1.6897	1.8895E-02	1.4324	5.9236E-02	1.1707
1/64		1.8455E-03	1.7660	6.8282E-03	1.4684	2.6093E-02	1.1828
1/128		5.2697E-04	1.8082	2.4369E-03	1.4864	1.1438E-02	1.1898
1/256		1.4844E-04	1.8278	8.6473E-04	1.4947	4.9994E-03	1.1940
1/512		4.1640E-05	1.8339	3.0612E-04	1.4981	2.1813E-03	1.1966
1/1024		1.1706E-05	1.8307	1.0830E-04	1.4991	9.5078E-04	1.1980
1/2048		3.3280E-06	1.8146	3.8328E-05	1.4985	4.1420E-04	1.1988
1/16	$3 - \cos(2x)$	1.6249E-02		4.2680E-02		1.1912E-01	
1/32		5.0240E-03	1.6934	1.5775E-02	1.4359	5.3240E-02	1.1619
1/64		1.4690E-03	1.7739	5.6826E-03	1.4731	2.3514E-02	1.1790
1/128		4.1646E-04	1.8186	5.6826E-03	1.4907	1.0318E-02	1.1883
1/256		1.1640E-04	1.8391	7.1584E-04	1.4981	4.5113E-03	1.1935
1/512		3.2413E-05	1.8444	2.5298E-04	1.5006	1.9685E-03	1.1964
1/1024		9.0742E-06	1.8367	8.9394E-05	1.5008	8.5805E-04	1.1980
1/2048		2.5962E-06	1.8054	3.1623E-05	1.4992	3.7380E-04	1.1988
EOC			1.8		1.5		1.2

In Table 4.2, we give the numerical results for the case when exact solution of the problem (4.1) is not known. In this Table 4.2, we determine the OC of the proposed method (4.44) by employing double computations on distinct grids $\tau_1 = \tau$ and $\tau_2 = \tau/2$. As observed form Table 4.2, the presented scheme (4.44) is computationally efficient and validates its consistency with the theoretical findings. Also indicates the stability of the proposed scheme as the OC remaining almost consistent up to two decimal places.

TABLE 4.2: Temporal direction computational errors and convergence order for **Case (i)** of Example 4.5.1 with decreasing temporal grids, $\delta = (2+\alpha)$, $p(x) = 3-\cos(2x)$, $q(x) = 1$, $F(u) = u$ and $M = 500$.

		$\alpha = 1.2$		$\alpha = 1.5$		$\alpha = 1.8$	
τ_1	τ_2	$\|U^\tau - U^{\tau/2}\|_\infty$	OC	$\|U^\tau - U^{\tau/2}\|_\infty$	OC	$\|U^\tau - U^{\tau/2}\|_\infty$	OC
$\frac{1}{64}$	$\frac{1}{128}$	4.7631E-04		2.7773E-03		1.1553E-02	
$\frac{1}{128}$	$\frac{1}{256}$	1.3731E-04	1.7944	9.9740E-04	1.4775	5.0912E-03	1.1822
$\frac{1}{256}$	$\frac{1}{512}$	3.9572E-05	1.7949	3.5596E-04	1.4864	2.2311E-03	1.1903
$\frac{1}{512}$	$\frac{1}{1024}$	1.1405E-05	1.7949	1.2660E-04	1.4915	9.7474E-04	1.1947
$\frac{1}{1024}$	$\frac{1}{2048}$	3.2874E-06	1.7947	4.4933E-05	1.4945	4.2514E-04	1.1971
$\frac{1}{2048}$	$\frac{1}{4096}$	9.4760E-07	1.7946	1.5928E-05	1.4962	1.8526E-04	1.1984
EOC			1.8		1.5		1.2

In Figure 4.2, we describe the surface plot of absolute errors for the nonosmooth exact solution $u(x,t) = t^\alpha \sin(2\pi x)$, $(x,t) \in [0,1] \times [0,1]$ using the scheme (4.44). Figure 4.2**(a)** represents the absolute error on uniform temporal meshes and the error obtained for nonuniform case is shown in Figure 4.2**(b)**. From these Figures 4.2**(a)** and 4.2**(b)**, we can observe the effects of nonsmooth solution near the singular point $t = 0$. In Figure 4.2**(a)**, the absolute error is blows-up near $t = 0$ but this behavior of error is tackled in Figure 4.2**(b)** by choosing more accumulated mesh near the singularity. Tables 4.3 and 4.4 showcase the maximum absolute errors and OC for nonsmooth solution by selecting $\delta = \alpha$ in **Case (i)** of Example 4.5.1 with Klein-Gorden and Sine-Gorden nonlinear problem (4.1)-(4.3). In these Tables 4.3 and 4.4, the desired computational outcomes can be expressed by taking different values of γ according to choices of α. From these Tables 4.3 and 4.4, one can note that the proposed scheme (4.44) is computationally accurate with theoretical OC and the numerical results are in good agreement with the expected accuracy $\min(3-\alpha, \gamma(\alpha-1))$.

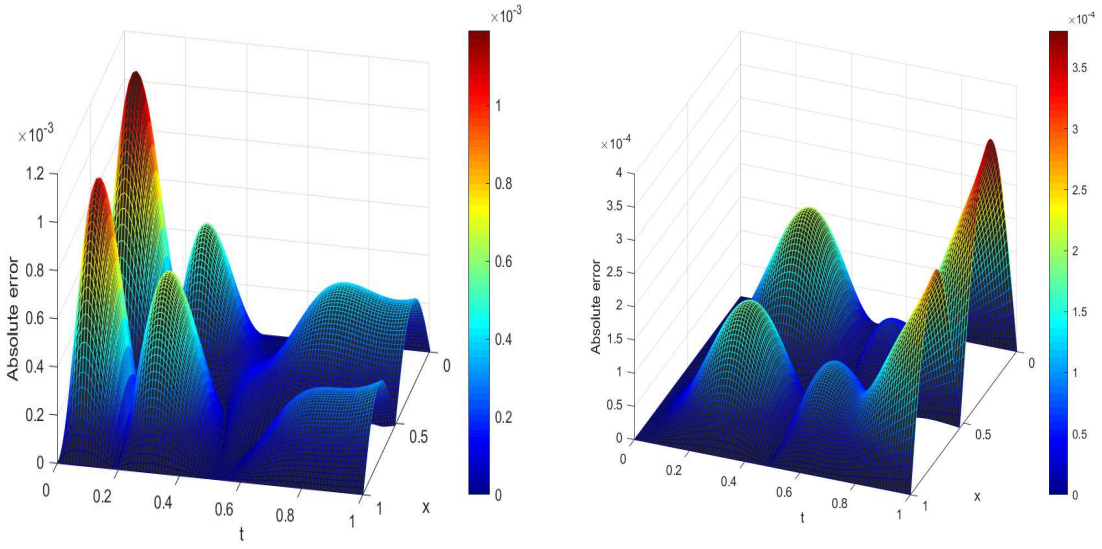

(a) Scheme (4.44) with $\gamma = 1$ and $M = N = 100$.

(b) Scheme (4.44) with $\gamma = 2$, $M = N = 100$.

FIGURE 4.2: Absolute error surfaces on both uniform **(a)** and nonuniform **(b)** meshes with $\alpha = 1.7$, $p(x) = 3 - \cos(2x)$, $q(x) = 1 - \sin(2x)$ and $(x, t) \in [0, 1] \times [0, 1]$.

TABLE 4.3: Temporal direction computational errors and convergence order for **Case (i)** of Example 4.5.1 with $\delta = \alpha$, $p(x) = 3 - \cos(2x)$, $q(x) = 1 - \sin(2x)$, $M = 2000$ and different choices of $F(u)$.

		$(\alpha,\gamma) = (1.5, 1)$		$(\alpha,\gamma) = (1.5, 3)$		$(\alpha,\gamma) = (1.7, 13/7)$	
τ_1	$F(u)$	$\|u^\tau - U^\tau\|_\infty$	OC	$\|u^\tau - U^\tau\|_\infty$	OC	$\|u^\tau - U^\tau\|_\infty$	OC
1/64	$u^3 - u$	8.7671E-03		1.6626E-03		3.5445E-03	
1/128		8.7332E-03	0.00558	5.6431E-04	1.5588	1.4088E-03	1.3311
1/256		7.4717E-03	0.22507	1.9588E-04	1.5265	5.6379E-04	1.3213
1/512		5.9862E-03	0.31980	6.8844E-05	1.5085	2.2667E-04	1.3146
1/1024		4.6079E-03	0.37752	2.4337E-05	1.5002	9.1389E-05	1.3105
1/2048		3.4531E-03	0.41623	8.6008E-06	1.5006	3.6893E-05	1.3087
1/4096		2.5415E-03	0.44223	3.0125E-06	1.5135	1.4885E-05	1.3095
1/64	$\sin(u)$	9.2518E-03		9.1913e-04		2.4481E-03	
1/128		7.7680E-03	0.25218	3.3823e-04	1.4423	9.9426E-04	1.3000
1/256		6.0768E-03	0.35423	1.2455e-04	1.4412	4.0251E-04	1.3046
1/512		4.5889E-03	0.40516	4.5605e-05	1.4495	1.6280E-04	1.3059
1/1024		3.4190E-03	0.42458	1.6554e-05	1.4620	6.5842E-05	1.3060
1/2048		2.5163E-03	0.44225	5.9460e-06	1.4772	2.6626E-05	1.3062
1/4096		1.8326E-03	0.45745	2.1024e-06	1.4999	1.0756E-05	1.3077
EOC			0.5		1.5		1.3

TABLE 4.4: Temporal direction computational errors and convergence order for **Case (i)** of Example 4.5.1 with $\delta = \alpha$, $p(x) = 3 - \cos(2x)$, $q(x) = 1 - \sin(2x)$, $F(u) = \sin(u)$, $M = 1000$ and different choices of parameter γ.

	$(\alpha, \gamma) = (1.4, 4)$		$(\alpha, \gamma) = (1.6, 7/3)$		$(\alpha, \gamma) = (1.8, 3/2)$	
τ	$\|u^\tau - U^\tau\|_\infty$	OC	$\|u^\tau - U^\tau\|_\infty$	OC	$\|u^\tau - U^\tau\|_\infty$	OC
1/32	1.7202E-03		3.9143E-03		8.3015E-03	
1/64	5.9505E-04	1.5315	1.4895E-03	1.3939	3.7592E-03	1.1429
1/128	2.0885E-04	1.5105	5.6976E-04	1.3864	1.6687E-03	1.1717
1/256	7.3456E-05	1.5075	2.1826E-04	1.3843	7.3326E-04	1.1863
1/512	2.5656E-05	1.5176	8.3447E-05	1.3871	3.2051E-04	1.1939
1/1024	8.8192E-06	1.5406	3.1761E-05	1.3936	1.3967E-04	1.1984
1/2048	2.9367E-06	1.5865	1.1986E-05	1.4059	6.0717E-05	1.2018
EOC		1.6		1.4		1.2

In Figure 4.3, we plot the surface of absolute error to make a comparison between uniform and nonuniform meshes for nonsmooth solution discussed in **Case (ii)** of Example 4.5.1. From the Figures (4.3)**(a)** and (4.3)**(b)**, it is clear that both surfaces exhibit different behavior near the singularity $t = 0$. In dealing with the weak initial singularity at time $t = 0$, we employ a graded mesh by selecting $\gamma > 1$ in the discretization of time derivative. Figure (4.3)**(b)** shows the plot of absolute error with nonuniform mesh $\gamma = 3$, indicating the effectiveness of graded meshes in the time discretization approach.

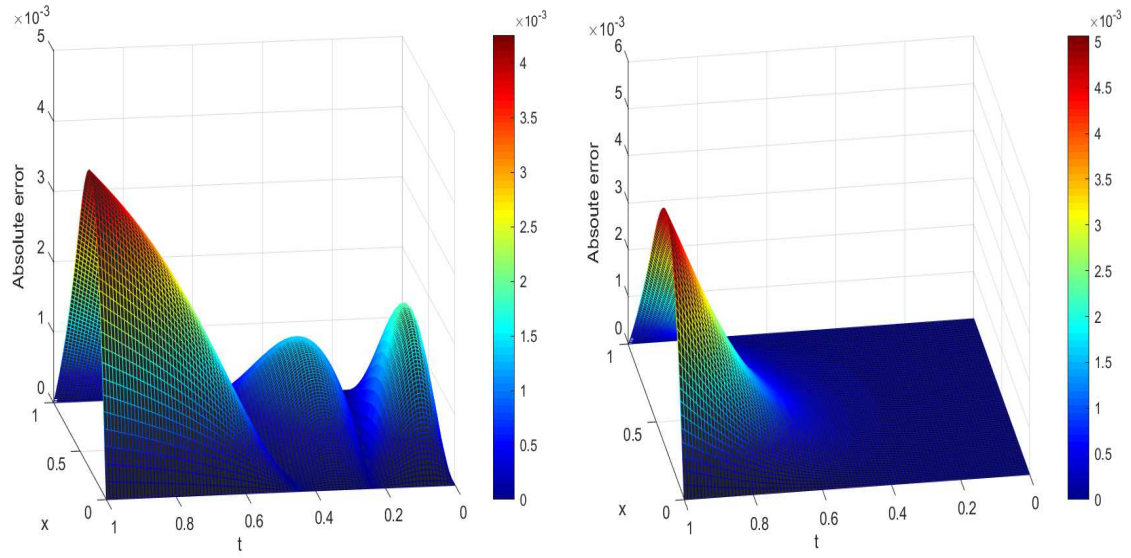

(a) Scheme (4.44) with $\gamma = 1$ and $M = N = 100$.

(b) Scheme (4.44) with $\gamma = 3$, $M = N = 100$.

FIGURE 4.3: Graph of absolute error on the uniform **(a)** (left) and nonuniform **(b)** (right) meshes for **Case (ii)** of Example 4.5.1 with $F(u) = \sin(u)$, $\delta = \alpha = 1.5$, $p(x) = 3 - \cos(2x)$ and $q(x) = 1 - \sin(2x)$.

In Figure 4.4, we plot the graphs of numerical results on uniform and nonuniform time meshes for **Case (i)** of Example 4.5.1. In Figures (4.4)**(a)** and (4.4)**(b)**, the computational solution is plotted varying values of (α, γ) at final time level $T = 1$. Table 4.5 displays the absolute errors and OC in space direction for nonsmooth solution with different values of (α, γ). We can observe that the scheme is second order accurate in space which is the expected OC. In Figure 4.5, we represent the numerical solutions for **Case(i)** of Example 4.5.1 with $\delta = \alpha$ on the domain $(x, t) \in [0, 2\pi] \times [0, 1]$. Figures (4.5)**(a)** and (4.5)**(b)** display the numerical results for uniform and nonuniform temporal meshes with $\gamma = 1$ and $\gamma = 4$, respectively. From Figure (4.5)**(a)**, it is clear that nonsmooth solutions exhibit blow-up behavior on uniform time meshes and this nature is handled in Figure (4.5)**(b)** by utilizing general temporal mesh.

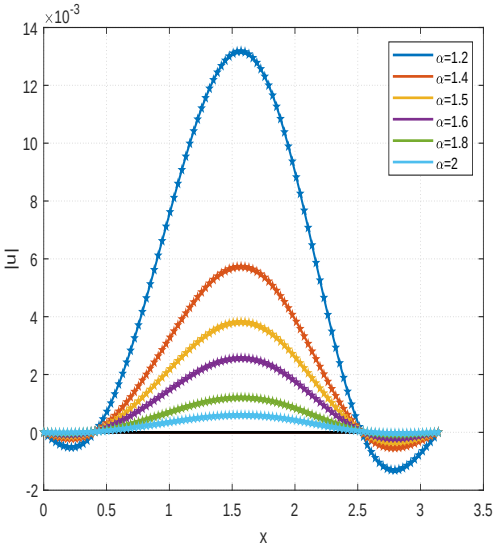

(a) Scheme (4.44) with $\gamma = 1$ and $M = N = 100$.

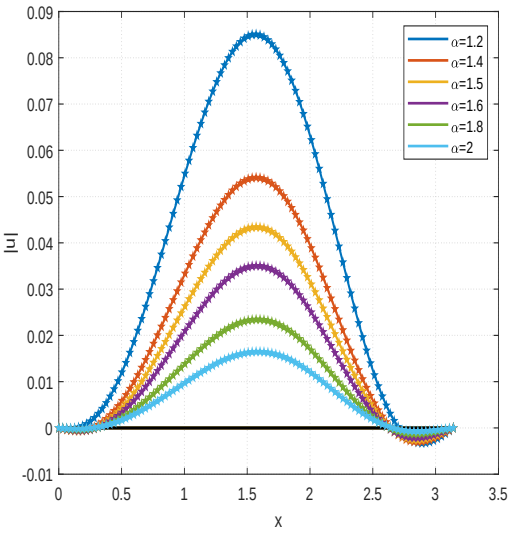

(b) Scheme (4.44) with $\gamma = 5$, $M = N = 100$.

FIGURE 4.4: Graph of $|u|$ on the uniform (left) and nonuniform meshes (right) at final time $T = 1$ for **case (i)** of Example 4.5.1 with $\delta = \alpha$, $F(u) = u^3 - u$, $p(x) = 3 - \cos(2x)$, $q(x) = 1 - \sin(2x)$ and different values of α.

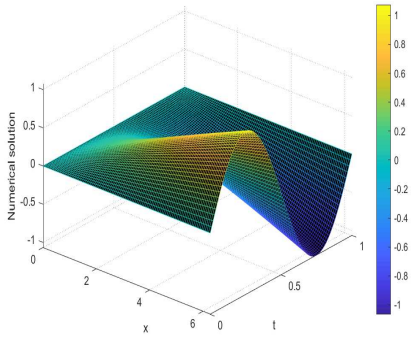

(a) For scheme (4.44) with $\gamma = 1$.

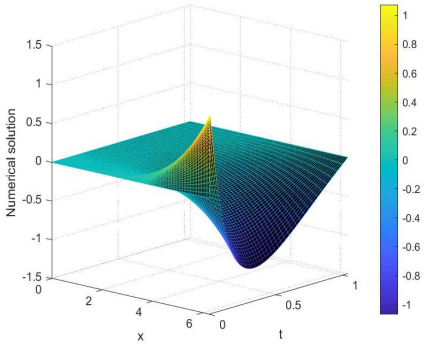

(b) For scheme (4.44) with $\gamma = 4$.

FIGURE 4.5: Comparison of numerical solutions for uniform (left) and nonuniform (right) temporal meshes with $p(x) = 3 - \cos(2x)$, $q(x) = 1 - \sin(2x)$, $\alpha = 1.1$ and $M = N = 100$.

TABLE 4.5: Spatial direction computational errors and convergence order for **Case (i)** of Example 4.5.1 with $\delta = \alpha$, $p(x) = 3 - \cos(2x)$, $q(x) = 1 - \sin(2x)$, $\tau = \frac{1}{7000}$ and different choices of parameters (α, γ).

		$(\alpha,\gamma) = (1.3, 4.7)$		$(\alpha,\gamma) = (1.5, 3)$		$(\alpha,\gamma) = (1.8, 1.18)$	
h	$F(u)$	$\|u^\tau - U^\tau\|_\infty$	OC	$\|u^\tau - U^\tau\|_\infty$	OC	$\|u^\tau - U^\tau\|_\infty$	OC
1/8	$u^3 - u$	8.2348E-03		7.4288E-03		6.1895E-03	
1/16		2.0153E-03	2.0307	1.8129E-03	2.0348	1.5019E-03	2.0431
1/32		5.0110E-04	2.0079	4.4996E-04	2.0104	3.7197E-04	2.0135
1/64		1.2495E-04	2.0037	1.1166E-04	2.0107	9.2069E-05	2.0144
1/128		3.1066E-05	2.0080	2.7231E-05	2.0357	2.2255E-05	2.0486
1/8	$\sin(u)$	8.2483E-03		7.5189E-03		6.3226E-03	
1/16		2.0279E-03	2.0241	1.8391E-03	2.0315	1.5353E-03	2.0420
1/32		5.0517E-04	2.0051	4.5651E-04	2.0103	3.8112E-04	2.0102
1/64		1.2642E-04	1.9986	1.1307E-04	2.0135	9.5198E-05	2.0012
1/128		3.1859E-05	1.9885	2.7343E-05	2.0479	2.3891E-05	1.9945
1/8	u	8.0231E-03		7.2981E-03		6.1334E-03	
1/16		1.9643E-03	2.0301	1.7816E-03	2.0343	1.4886E-03	2.0427
1/32		4.8850E-04	2.0076	4.4226E-04	2.0102	3.6879E-04	2.0131
1/64		1.2186E-04	2.0031	1.0978E-04	2.0102	9.1374E-05	2.0129
1/128		3.0346E-05	2.0056	2.6811E-05	2.0338	2.2178E-05	2.0426
EOC			2.00		2.00		2.00

In Tables 4.6, we display the rate of convergence and maximum absolute errors for nonsmooth exact solution with uniform and nonuniform temporal meshes. In this Table 4.6, first we fix $M = 2000$ and vary values of N to get the temporal accuracy. From Table 4.6, we can observe that the scheme does not achieve desired accuracy for uniform time meshes (i.e.$\gamma = 1$). However the scheme is well accurate with the expected convergence order using the nonuniform time meshes ($\gamma > 1$) for same values of $\alpha = 1.3,\ 1.5,\ 1.8$. The obtained results are in good agreement with the theoretical order i.e. $\min(3 - \alpha, \gamma(\alpha - 1))$. Table 4.7 shows the errors and OC in

space direction for the nonsmooth solution of problem 4.5.1. Table 4.7 expresses that the scheme (4.44) is numerically efficient and achieves second-order accuracy in space. In Table 4.7, the numerical results are given for $p(x) = 3 - \cos(2x)$, $q(x) = 2 - \sin(3x)$ with fix $N = 5000$ and varying M. In Table 4.8, we display the errors on L_∞-norm and corresponding rate of convergence for discontinuous initial data [131]. To calculate the numerical accuracy, first we considered a reference solution with $h_{ref} = 2^{-5}$ and then vary $N = [2^3,\ 2^4,\ 2^5,\ 2^6,\ 2^7]$. Table 4.8 presents the numerical results for $t = 0.005$ and 0.001 as we are interested in the efficiency of the scheme near small t. We observe that the scheme is $(3 - \alpha)$-order accurate for both constant and variable coefficients of problem (4.1) with nonsmooth initial data.

TABLE 4.6: Temporal direction computational errors and convergence order for **Case (ii)** of Example 4.5.1 with $p(x) = 3-\cos(2x)$, $q(x) = 2-\sin(3x)$, $M = 2000$ and different choices of parameters (α, γ).

	(α,γ)	$(1.3,1)$		$(1.5,1)$		$(1.8,1)$	
τ		$\|u^\tau - U^\tau\|_\infty$	OC	$\|u^\tau - U^\tau\|_\infty$	OC	$\|u^\tau - U^\tau\|_\infty$	OC
1/32		3.8734E-02		1.9552E-02		5.5707E-02	
1/64		3.0930E-02	0.32461	1.5566E-02	0.32892	3.3345E-02	0.74037
1/128		2.4871E-02	0.31454	1.2003E-02	0.37506	1.9511E-02	0.77321
1/256		1.9959E-02	0.31746	9.2031E-03	0.38315	1.1209E-02	0.79957
1/512		1.5949E-02	0.32358	7.0213E-03	0.39040	6.3291E-03	0.82462
1/1024		1.2702E-02	0.32838	5.2791E-03	0.41143	3.5055E-03	0.85241
EOC			0.3		0.5		0.8
	(α,γ)	$(1.3,17/3)$		$(1.5,3)$		$(1.8,2)$	
		$\|u^\tau - U^\tau\|_\infty$	OC	$\|u^\tau - U^\tau\|_\infty$	OC	$\|u^\tau - U^\tau\|_\infty$	OC
1/32		4.5212E-03		5.2846E-03		2.7083E-02	
1/64		1.4157E-03	1.6751	1.8227E-03	1.5357	1.2647E-02	1.0985
1/128		4.4215E-04	1.6789	6.3736E-04	1.5159	5.7603E-03	1.1346
1/256		1.3778E-04	1.6821	2.2446E-04	1.5057	2.5783E-03	1.1597
1/512		4.2806E-05	1.6865	7.9282E-05	1.5014	1.1379E-03	1.1801
1/1024		1.3252E-05	1.6917	2.8009E-05	1.5011	4.9598E-04	1.1980
EOC			1.7		1.5		1.2

In Figure 4.6, we plot the comparison of theoretical OC with rate of convergence for nonsmooth exact solution by selecting suitable grading parameter γ. Figure 4.6 is plotted for nonsmooth solution defined in **Case (ii)** of Example 4.5.1 with variable coefficients $p(x) = 3-\cos(2x)$, $q(x) = 2-\sin(3x)$, for fix space step-size $h = 1/2000$ and varying temporal steps $\tau = 2^{-n}$ $(n = 8,\ 9,\ 10,\ 11)$. Figure 4.6 confirms that the scheme (4.44) has almost similar convergence rate for nonsmooth solutions as presented in the theoretical part i.e. $N^{-\min(3-\alpha,\gamma(\alpha-1))}$, $1 < \alpha < 2$.

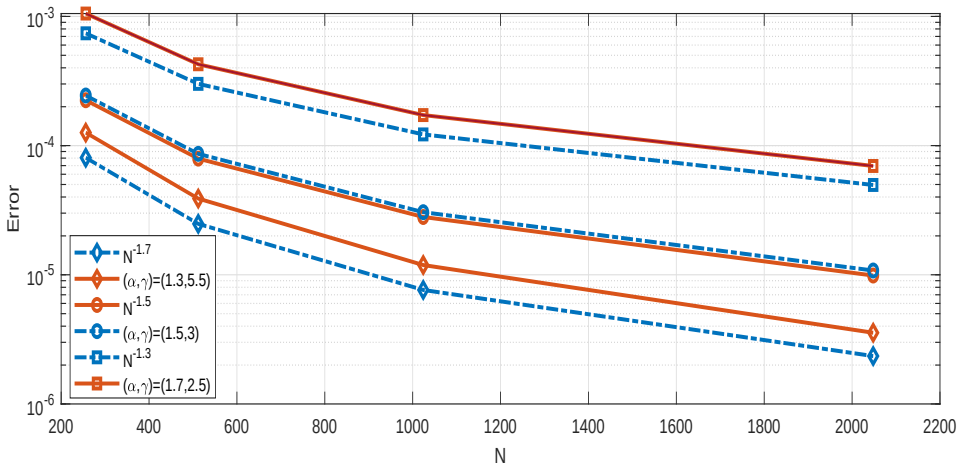

FIGURE 4.6: Convergence rate in time direction for **Case (ii)** of Example 4.5.1 with $F(u) = u$, $p(x) = 3 - \cos(2x)$, $q(x) = 2 - \sin(3x)$, $\tau = \frac{1}{256}, \frac{1}{512}, \frac{1}{1024}, \frac{1}{2048}$ and $h = 0.0005$.

TABLE 4.7: Spatial direction computational errors and convergence order for **Case (ii)** of Example 4.5.1 with $p(x) = 3 - \cos(2x)$, $q(x) = 2 - \sin(3x)$, $\tau = \frac{1}{5000}$ and different choices of parameters (α, γ).

	$(\alpha,\gamma) = (1.3, 17/3)$		$(\alpha,\gamma) = (1.5, 3)$		$(\alpha,\gamma) = (1.7, 1.2)$		
h	$\|u^\tau - U^\tau\|_\infty$	OC	$\|u^\tau - U^\tau\|_\infty$	OC	$\|u^\tau - U^\tau\|_\infty$	OC	CPU(s)
1/8	1.3503E-02		1.2861E-02		1.2115E-02		31.66963
1/16	3.3130E-03	2.0271	3.1465E-03	2.0312	2.9531E-03	2.0365	63.27619
1/32	8.2532E-04	2.0051	7.8106E-04	2.0103	7.3592E-04	2.0046	96.84626
1/64	2.0702E-04	1.9952	1.9350E-04	2.0131	1.8607E-04	1.9837	143.5895
EOC		2.00		2.00		2.00	

TABLE 4.8: Temporal direction computational errors and convergence order for **Case (iii)** of Example 4.5.1 with $F(u) = u^3 - u$, $\alpha = 1.5$, $h = 2^{-5}$ and different choices of coefficients $p(x)$, $q(x)$.

		$t \backslash (p(x), q(x))$	$(3 - \cos(2x), 2 - \sin(3x))$		$(1, 1)$	
τ_1	τ_2		$\|U^{\tau_1} - U^{\tau_2}\|_\infty$	OC	$\|U^{\tau_1} - U^{\tau_2}\|_\infty$	OC
$\frac{1}{8}$	$\frac{1}{16}$		2.8650E-02		1.6492E-02	
$\frac{1}{16}$	$\frac{1}{32}$	0.005	1.3921E-02	1.0413	7.4749E-03	1.1416
$\frac{1}{32}$	$\frac{1}{64}$		6.2423E-03	1.1571	3.0794E-03	1.2794
$\frac{1}{64}$	$\frac{1}{128}$		2.6179E-03	1.2537	1.1916E-03	1.3697
$\frac{1}{128}$	$\frac{1}{256}$		1.0287E-03	1.3476	4.4012E-04	1.4369
$\frac{1}{8}$	$\frac{1}{16}$		4.0262E-03		1.6674E-03	
$\frac{1}{16}$	$\frac{1}{32}$	0.001	1.8927E-03	1.0890	7.9558E-04	1.0675
$\frac{1}{32}$	$\frac{1}{64}$		7.5238E-04	1.3309	3.1739E-04	1.3258
$\frac{1}{64}$	$\frac{1}{128}$		2.7729E-04	1.4401	1.1371E-04	1.4809
$\frac{1}{128}$	$\frac{1}{256}$		9.9727E-05	1.4753	4.0401E-05	1.4929

In Figure 4.7, we demonstrate the approximate solution for **Case (iii)** of Example 4.5.1 with different values of $\alpha = 1.3$ 1.6, 1.8. In **Case (iii)** the exact solution is not known in compact form, then we calculate the reference solution by using $h_{ref} = 2^{-5}$ in proposed scheme (4.44). The computational outcomes for **Case (iii)** with varying $p(x)$ and $q(x)$ are displayed in Table 4.8. We are specifically interested in conditions where the value of t is small. Therefore, we show the graph of numerical results for $t = 0.1$ and $t = 0.01$ in Figure 4.7. Additionally, as α approaches two, the decay of the solution slows down (for values of t that are close to zero).

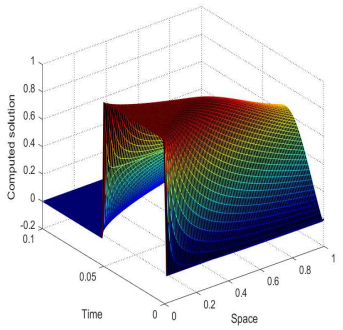

(a) $\alpha = 1.3$ and $t = 0.1$.

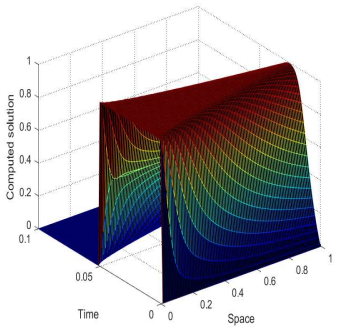

(b) $\alpha = 1.6$ and $t = 0.1$.

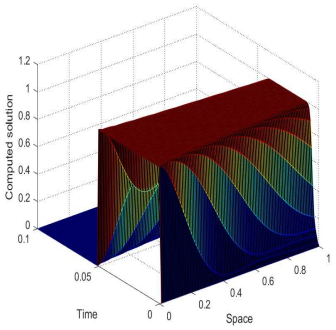

(c) $\alpha = 1.8$ and $t = 0.1$.

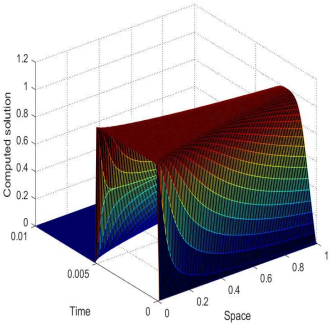

(d) $\alpha = 1.3$ and $t = 0.01$.

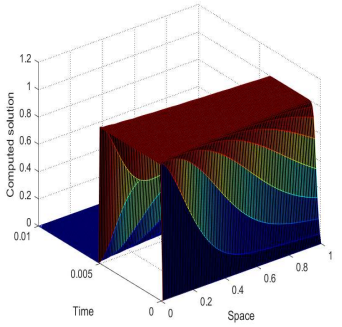

(e) $\alpha = 1.6$ and $t = 0.01$.

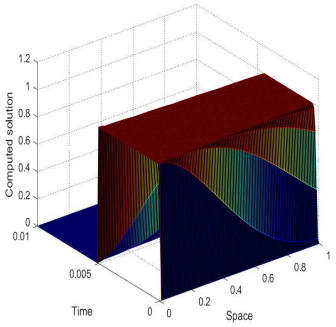

(f) $\alpha = 1.8$ and $t = 0.01$.

FIGURE 4.7: Graphs of numerical solution for **Case (iii)** of Example 4.5.1 using the difference scheme (4.44) with $M = N = 100$ and different values of α.

Example 4.5.2. Consider the following Klein-Gorden and Sine-Gorden time-fractional Telegraph equation with variable coefficients in both one and two-dimensions

$$ {}^{C}\mathcal{D}^{\alpha}_{0,t}u(X_{\widehat{l}},t) + {}^{C}\mathcal{D}^{\alpha-1}_{0,t}u(X_{\widehat{l}},t) + q(X_{\widehat{l}})F\big(u(X_{\widehat{l}},t)\big) = \frac{\partial}{\partial X_{\widehat{l}}}\left(p(X_{\widehat{l}})\,\frac{\partial u(X_{\widehat{l}},t)}{\partial X_{\widehat{l}}}\right) + f(X_{\widehat{l}},t), $$

$$ \widehat{l} = 1, 2,\ X_1 \equiv x,\ X_2 \equiv (x, y),\ (X_{\widehat{l}}, t) \in \Omega \times (0, T]. $$

In this Example 4.5.2, we consider two cases (4.97) and (4.98), corresponding to one and two-dimensions, respectively. Tables 4.9 and 4.10, display the numerical results in time and space directions, respectively for the case (4.97) using the scheme (4.44).

Table 4.9 represent the absolute errors and rate of convergence in the time direction, fixing $M = 2000$ and varying N. In Tables 4.9 and 4.10, we represent the results for $p(x) = 3 - \cos(2x)$, $q(x) = 1 - \sin(3x)$ with different values of (α, γ). Table 4.11 shows the computational results in time for two-dimensional case (4.98) of Example 4.5.2. For the two-dimensional case, we use ADI scheme (4.64)-(4.66) to calculate the errors and corresponding OC. From these Tables 4.9, 4.10 and 4.11, we observe that the numerical results are in good agreements with EOC.

$$
\text{(a)}\begin{cases}
u(x,t) = t^{\alpha}\exp\left(\frac{-(x-0.5)^2}{0.02}\right), \quad x \in [0,1],\ t \in (0,1], \\
u(x,0) = u_t(x,0) = 0, \quad x \in [0,1], \\
u(0,t) = t^{\alpha}\exp\left(\frac{-(0.5)^2}{0.02}\right), \quad t \in (0,1], \\
u(1,t) = t^{\alpha}\exp\left(\frac{-(0.5)^2}{0.02}\right), \quad t \in (0,1], \\
f(x,t) = \Gamma(\alpha+1)(1+t)\exp\left(\frac{-(x-0.5)^2}{0.02}\right) + 100t^{\alpha}(2(x-0.5)\sin(2x) \\
\qquad +(3-\cos(2x)) - \frac{1}{0.01}(x-0.5)^2(3-\cos(2x)))\exp\left(\frac{-(x-0.5)^2}{0.02}\right) \\
\qquad +(1-\sin(3x))F(u(x,t)).
\end{cases}
\tag{4.97}
$$

$$
\text{(b)}\begin{cases}
u(x,y,t) = t^3\exp\left(\frac{-(x-5)^2}{\beta} + \frac{-(y-5)^2}{\beta}\right), \quad (x,y) \in [0,10]\times[0,10],\ t \in (0,1], \\
u(x,y,0) = u_t(x,y,0) = 0 \quad (x,y) \in [0,10]\times[0,10], \\
u(0,y,t) = u(10,y,t) = t^3\exp\left(\frac{-5^2}{\beta} + \frac{-(y-5)^2}{\beta}\right), \quad y \in [0,10],\ t \in (0,1], \\
u(x,0,t) = u(x,10,t) = t^3\exp\left(\frac{-(x-5)^2}{\beta} + \frac{-5^2}{\beta}\right), \quad x \in [0,10],\ t \in (0,1], \\
u(0,0,t) = u(10,10,t) = t^3\exp\left(\frac{-50}{\beta}\right), \quad t \in (0,1] \\
f(x,y,t) = \left(\frac{6}{\Gamma(3-\alpha)}t^{2-\alpha} + \frac{6}{\Gamma(4-\alpha)}t^{3-\alpha} + \frac{4}{\beta}t^3 - \left(\frac{2}{\beta}\right)^2 t^3(x-5)^2\right. \\
\qquad \left. -\left(\frac{2}{\beta}\right)^2 t^3(y-5)^2\right)\exp\left(\frac{-(x-5)^2}{\beta} + \frac{-(y-5)^2}{\beta}\right) + q(x,y)F(u(x,y,t)).
\end{cases}
\tag{4.98}
$$

TABLE 4.9: Temporal direction computational errors and convergence order for 1D case (4.97) of Example 4.5.2 with $p(x) = 3 - \cos(2x)$, $q(x) = 1 - \sin(3x)$, $M = 2000$ and different choices of parameter (α, γ).

		$(\alpha,\gamma) = (1.4, 4)$		$(\alpha,\gamma) = (1.6, 7/3)$		$(\alpha,\gamma) = (1.8, 3/2)$	
τ	$F(u)$	$\|u^\tau - U^\tau\|_\infty$	OC	$\|u^\tau - U^\tau\|_\infty$	OC	$\|u^\tau - U^\tau\|_\infty$	OC
1/16	$u^3 - u$	9.6733E-04		1.6553E-03		2.4445E-03	
1/32		3.0614E-04	1.6598	5.8611E-04	1.4978	1.0893E-03	1.1661
1/64		9.8835E-05	1.6311	2.0878E-04	1.4892	4.7846E-04	1.1870
1/128		3.2306E-05	1.6132	7.5732E-05	1.4630	2.0872E-04	1.1968
1/256		1.0594E-05	1.6086	2.7850E-05	1.4432	9.0792E-05	1.2009
1/512		3.4606E-06	1.6142	1.0317E-05	1.4327	3.9434E-05	1.2031
1/16	$\sin(u)$	9.5507E-04		1.6431E-03		2.4343E-03	
1/32		3.0215E-04	1.6604	5.8322E-04	1.4943	1.0864E-03	1.1639
1/64		9.7644E-05	1.6296	2.0767E-04	1.4898	4.7773E-04	1.1853
1/128		3.1962E-05	1.6112	7.5374E-05	1.4621	2.0847E-04	1.1963
1/256		1.0494E-05	1.6068	2.7729E-05	1.4427	9.0699E-05	1.2007
1/512		3.4287E-06	1.6138	1.0274E-05	1.4324	3.9396E-05	1.2030
EOC			1.6		1.4		1.2

TABLE 4.10: Spatial direction computational errors and convergence order for 1D case (4.97) of Example 4.5.2 with $p(x) = 3 - \cos(2x)$, $q(x) = 1 - \sin(3x)$, $\tau = \frac{1}{1000}$ and different choices of parameter (α, γ).

		$(\alpha,\gamma) = (1.3, 17/3)$		$(\alpha,\gamma) = (1.5, 3)$		$(\alpha,\gamma) = (1.8, 3/2)$	
h	$F(u)$	$\|u^\tau - U^\tau\|_\infty$	OC	$\|u^\tau - U^\tau\|_\infty$	OC	$\|u^\tau - U^\tau\|_\infty$	OC
1/16	$u^3 - u$	3.4503E-02		3.4359E-02		3.4223E-02	
1/32		8.2311E-03	2.0675	8.1971E-03	2.0675	8.1696E-03	2.0666
1/64		2.0334E-03	2.0172	2.0253E-03	2.0170	2.0233E-03	2.0136
1/128		5.0535E-04	2.0086	5.0354E-04	2.0079	5.0788E-04	1.9942
1/16	$\sin(u)$	3.4573E-02		3.4428E-02		3.4291E-02	
1/32		8.2486E-03	2.0674	8.2142E-03	2.0674	8.1861E-03	2.0666
1/64		2.0378E-03	2.0171	2.0295E-03	2.0170	2.0272E-03	2.0137
1/128		5.0645E-04	2.0085	5.0462E-04	2.0079	5.0869E-04	1.9947
EOC			2.00		2.00		2.00

TABLE 4.11: Temporal direction computational errors and convergence order for 2D case (4.98) of Example 4.5.2 with $p(x) = 1$, $q(x) = 3-\sin(2(x+y))$, $\beta = 1000$, $M_1 = 25$, $M_2 = 25$ and different choices of parameter α.

		$\alpha = 1.25$		$\alpha = 1.5$		$\alpha = 1.8$	
τ	$F(u)$	$\|u^\tau - U^\tau\|_\infty$	OC	$\|u^\tau - U^\tau\|_\infty$	OC	$\|u^\tau - U^\tau\|_\infty$	OC
1/8	$\sin(u)$	2.3612E-02		4.2967E-02		9.8346E-02	
1/16		6.4007E-03	1.8832	1.4157E-02	1.6017	4.1262E-02	1.2531
1/32		1.7448E-03	1.8752	4.7177E-03	1.5854	1.7573E-02	1.2314
1/64		4.8170E-04	1.8568	1.5928E-03	1.5665	7.5507E-03	1.2187
1/128		1.3508E-04	1.8343	5.4409E-04	1.5497	3.2615E-03	1.2111
1/256		3.9125E-05	1.7876	1.8767E-04	1.5356	1.4133E-03	1.2065
1/8	$u^3 - u$	6.2593E-02		7.4783E-02		1.3762E-01	
1/16		1.9646E-02	1.6718	2.6040E-02	1.5220	5.9020E-02	1.2215
1/32		5.7218E-03	1.7797	8.9216E-03	1.5454	2.5603E-02	1.2049
1/64		1.6113E-03	1.8282	3.0402E-03	1.5531	1.1133E-02	1.2015
1/128		4.4578E-04	1.8538	1.0377E-03	1.5507	4.8424E-03	1.2010
1/256		1.2272E-04	1.8610	3.5628E-04	1.5424	2.1065E-03	1.2009
1/8	u	3.2251E-02		4.6637E-02		9.9393E-02	
1/16		8.7921E-03	1.8751	1.5087E-02	1.6281	4.1255E-02	1.2686
1/32		2.3690E-03	1.8919	4.9356E-03	1.6120	1.7451E-02	1.2412
1/64		6.3687E-04	1.8952	1.6367E-03	1.5925	7.4660E-03	1.2249
1/128		1.7183E-04	1.8900	5.5033E-04	1.5724	3.2162E-03	1.2150
1/256		4.7454E-05	1.8564	1.8740E-04	1.5542	1.3914E-03	1.2089
EOC			1.85		1.50		1.20

In Figure 4.8, we display the errors comparison on uniform and nonuniform temporal meshes for nonsmooth exact solutions. Figure (4.8)**(a)** represents the maximum absolute error plot for 1D case (4.97) of Example 4.5.2 with $p(x) = 3 - \cos(2x)$, $q(x) = 1 - \sin(3x)$ on the domain $[0, 1] \times [0, 1]$. In Figure (4.8)**(b)**, we demonstrate the errors on L_∞ norm for nonsmooth solution in **Case (i)** of Example 4.5.1 with $p(x) = 3 - \cos(2x)$, $q(x) = 1 - \sin(2x)$, $F(u) = u^3 - u$ on the domain $[0, \pi] \times [0, 1]$.

From Figure 4.8, we observe that the impact of employing nonuniform temporal meshes on nonsmooth exact solutions.

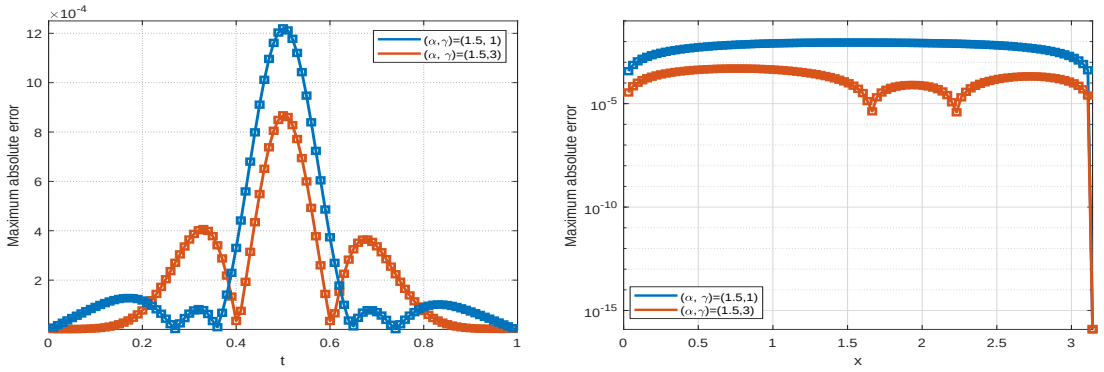

(a) For scheme (4.44) with $M = N = 100$.

(b) For scheme (4.44) with $M = N = 100$.

FIGURE 4.8: Comparison of absolute errors on uniform and nonuniform mesh for 1D case of Example 4.5.2 (left) and **Case (i)** (with $\delta = \alpha$) of Example 4.5.1 (right) at final time $T = 1$.

Example 4.5.3. Consider the following Klein-Gorden and Sine-Gorden multi-term TFDW equation with variable coefficients on the domain $\Omega \times [0, T] = [0, 1] \times [0, 1]$

$$\begin{cases} \sum_{r=0}^{2} \omega_r \, {}^{C}\mathcal{D}_{0,t}^{\alpha_r} u(x,t) + q(x)F(u(x,t)) = \frac{\partial}{\partial x}\left((3-\cos(2x))\frac{\partial u(x,t)}{\partial x}\right) + f(x,t), \\ u(x,0) = 0, \quad u_t(x,0) = 0, \quad x \in \Omega, \\ u(0,t) = t^\theta, \quad u(1,t) = t^\theta \sec h^2(1), \quad (x,t) \in \partial\Omega \times (0,T], \end{cases}$$

with the exact solution $u(x,t) = t^\theta \sec h^2(x)$, $(x,t) \in [0,1] \times [0,1]$. Subsequently, the associated source term is described as:

$$\begin{aligned} f(x,t) =& \frac{\Gamma(\theta+1)}{\Gamma(\theta+1-\alpha)} t^{\theta-\alpha_r} \sec h^2(x) + q(x)F(u(x,t)) + 2t^\theta [2\sin(2x)\tanh(x)\sec h^2(x) \\ & - 2(3-\cos(2x))\sec h^2(x)\tanh^2(x) + (3-\cos(2x))\sec h^4(x)]. \end{aligned}$$

We solve this Example 4.5.3 employing the scheme (4.55). In Tables 4.12, 4.13, 4.14, 4.15, 4.16, we display the computational results for both time and spatial directions. Tables 4.12 and 4.14 demonstrate the rate of convergence and errors in temporal direction for Sine-Gorden and Klein-Gorden problem 4.5.3 with smooth exact solution. However, Tables 4.13 and 4.15 display the time direction numerical simulation with nonsmooth exact solution utilizing graded meshes for the Sine-Gorden and Klein-Gorden Example 4.5.3, respectively. In Table 4.16, we give the numerical results in spatial direction for the Klein-Gorden problem 4.5.3 with nonsmooth exact solution by using different values of grading parameter γ. In these Tables 4.12-4.16, we choose $\omega_r = 1$ for $r = 0, 1, 2$ and different values of α_0, α_1, α_2 and $p(x)$, $q(x)$. The rate of convergence in each table compares with EOC. One can note that the scheme has good accuracy and in agreement with theoretical findings.

TABLE 4.12: Temporal direction computational errors and convergence order for **Case (i)** of Example 4.5.3 with $\theta = 4$, $p(x) = 3 - \cos(2x)$, $q(x) = 3 - \sin(2x)$, $F(u) = \sin(u)$, $M = 2000$ and different choices of $(\alpha_0, \alpha_1, \alpha_2)$.

	$(\alpha_0, \alpha_1, \alpha_2) = (\frac{4}{3}, \frac{5}{4}, \frac{6}{5})$		$(\alpha_0, \alpha_1, \alpha_2) = (\frac{5}{4}, \frac{23}{20}, \frac{11}{10})$		$(\alpha_0, \alpha_1, \alpha_2) = (\frac{5}{3}, \frac{3}{2}, \frac{4}{3})$		
τ	$\|u^\tau - U^\tau\|_\infty$	OC	$\|u^\tau - U^\tau\|_\infty$	OC	$\|u^\tau - U^\tau\|_\infty$	OC	CPU(s)
1/16	5.4820E-03		4.2087E-03		1.4791E-02		16.9184
1/32	1.7499E-03	1.6474	1.2591E-03	1.7410	6.5011E-03	1.1860	36.7088
1/64	5.5378E-04	1.6599	3.7688E-04	1.7402	2.7114E-03	1.2616	64.0802
1/128	1.7390E-04	1.6711	1.1166E-04	1.7550	1.0961E-03	1.3066	107.347
1/256	5.4550E-05	1.6726	3.2917E-05	1.7622	4.3738E-04	1.3255	183.310
1/512	1.7227E-05	1.6629	9.7599E-06	1.7539	1.7376E-04	1.3317	330.443
EOC		1.6667		1.75		1.3333	

TABLE 4.13: Temporal direction computational errors and convergence order for **Case (i)** of Example 4.5.3 with $\theta = \frac{3}{2}$, $p(x) = 3 - \cos(2x)$, $q(x) = 3 - \sin(2x)$, $F(u) = \sin(u)$, $M = 2000$ and different choices of $(\alpha_0, \alpha_1, \alpha_2, \gamma)$.

	$(\alpha_0,\alpha_1,\alpha_2) = (\frac{4}{3}, \frac{5}{4}, \frac{6}{5})$		$(\alpha_0,\alpha_1,\alpha_2) = (\frac{5}{4}, \frac{23}{20}, \frac{11}{10})$		$(\alpha_0,\alpha_1,\alpha_2) = (\frac{5}{3}, \frac{3}{2}, \frac{4}{3})$		
	$\gamma = 3$		$\gamma = 3.22$		$\gamma = 2.67$		
τ	$\|u^\tau - U^\tau\|_\infty$	OC	$\|u^\tau - U^\tau\|_\infty$	OC	$\|u^\tau - U^\tau\|_\infty$	OC	CPU(s)
1/32	6.7120E-04		7.5749E-04		2.4923E-03		18.9389
1/64	1.7356E-04	1.9513	1.9513E-04	1.9568	1.1011E-03	1.1786	42.3101
1/128	4.5751E-05	1.9236	5.0188E-05	1.9590	4.5663E-04	1.2698	78.4787
1/256	1.2500E-05	1.8719	1.3134E-05	1.9341	1.8399E-04	1.3114	142.289
1/512	3.6160E-06	1.7894	3.5626E-06	1.8823	7.3368E-05	1.3264	265.764
1/1024	1.1501E-06	1.6526	1.0504E-06	1.7620	2.9152E-05	1.3316	579.894
EOC		1.6667		1.75		1.3333	

TABLE 4.14: Temporal direction computational errors and convergence order for **Case (i)** of Example 4.5.3 with $\theta = 4$, $p(x) = 3 - \cos(2x)$, $q(x) = 1 - \sin(2x)$, $F(u) = u^3 - u$, $M = 2000$ and different choices of $(\alpha_0, \alpha_1, \alpha_2)$.

	$(\alpha_0,\alpha_1,\alpha_2) = (\frac{4}{3}, \frac{5}{4}, \frac{6}{5})$		$(\alpha_0,\alpha_1,\alpha_2) = (\frac{5}{4}, \frac{23}{20}, \frac{11}{10})$		$(\alpha_0,\alpha_1,\alpha_2) = (\frac{5}{3}, \frac{3}{2}, \frac{4}{3})$		
τ	$\|u^\tau - U^\tau\|_\infty$	OC	$\|u^\tau - U^\tau\|_\infty$	OC	$\|u^\tau - U^\tau\|_\infty$	OC	CPU(s)
1/16	5.4599E-03		4.2246E-03		1.5155E-02		13.7449
1/32	1.8998E-03	1.5230	1.4286E-03	1.5642	6.8266E-03	1.1505	29.5159
1/64	6.2290E-04	1.6088	4.4814E-04	1.6726	2.8827E-03	1.2437	51.3131
1/128	1.9767E-04	1.6559	1.3484E-04	1.7327	1.1749E-03	1.2948	85.3112
1/256	6.1877E-05	1.6756	3.9822E-05	1.7596	4.7133E-04	1.3178	146.558
1/512	1.9371E-05	1.6755	1.1770E-05	1.7585	1.8789E-04	1.3269	264.414
EOC		1.6667		1.75		1.3333	

TABLE 4.15: Temporal direction computational errors and convergence order for **Case (i)** of Example 4.5.3 with $\theta = \frac{3}{2}$, $p(x) = 3 - \cos(2x)$, $q(x) = 1 - \sin(2x)$, $F(u) = u^3 - u$, $M = 2000$ and different choices of $(\alpha_0, \alpha_1, \alpha_2, \gamma)$.

	$(\alpha_0,\alpha_1,\alpha_2) = (\frac{4}{3},\frac{5}{4},\frac{6}{5})$		$(\alpha_0,\alpha_1,\alpha_2) = (\frac{5}{4},\frac{23}{20},\frac{11}{10})$		$(\alpha_0,\alpha_1,\alpha_2) = (\frac{5}{3},\frac{3}{2},\frac{4}{3})$		
	$\gamma = 3$		$\gamma = 3.22$		$\gamma = 2.67$		
τ	$\|u^\tau - U^\tau\|_\infty$	OC	$\|u^\tau - U^\tau\|_\infty$	OC	$\|u^\tau - U^\tau\|_\infty$	OC	CPU(s)
1/32	1.4316E-03		1.6879E-03		2.8141E-03		20.7924
1/64	3.5387E-04	2.0163	4.1528E-04	2.0231	1.2096E-03	1.2181	48.2781
1/128	8.9409E-05	1.9847	1.0384E-04	1.9997	4.9315E-04	1.2944	91.2881
1/256	2.3238E-05	1.9440	2.6429E-05	1.9742	1.9689E-04	1.3246	166.990
1/512	6.3696E-06	1.8672	6.9878E-06	1.9192	7.8090E-05	1.3342	314.496
1/1024	1.9700E-06	1.6930	2.0524E-06	1.7675	3.0927E-05	1.3363	638.506
EOC		1.6667		1.75		1.3333	

TABLE 4.16: Spatial direction computational errors and convergence order for Example 4.5.3 with $p(x) = 3 - \cos(2x)$, $q(x) = 1 - \sin(2x)$, $F(u) = u^3 - u$, $\tau = \frac{1}{7000}$ and different choices of parameter $(\alpha_0, \alpha_1, \alpha_2, \gamma)$.

	$(\alpha_0,\alpha_1,\alpha_2) = (\frac{4}{3},\frac{5}{4},\frac{6}{5})$		$(\alpha_0,\alpha_1,\alpha_2) = (\frac{5}{4},\frac{23}{20},\frac{11}{10})$		$(\alpha_0,\alpha_1,\alpha_2) = (\frac{5}{3},\frac{3}{2},\frac{4}{3})$		
	$\gamma = 3$		$\gamma = 3.22$		$\gamma = 2.67$		
τ	$\|u^\tau - U^\tau\|_\infty$	OC	$\|u^\tau - U^\tau\|_\infty$	OC	$\|u^\tau - U^\tau\|_\infty$	OC	CPU(s)
1/16	7.0918E-03		7.0892E-03		7.1224E-03		2302.00
1/32	1.8643E-03	1.9275	1.8640E-03	1.9272	1.8681E-03	1.9308	4616.61
1/64	4.7738E-04	1.9654	4.7736E-04	1.9653	4.7784E-04	1.9670	6968.95
1/128	1.2075E-04	1.9831	1.2075E-04	1.9830	1.2080E-04	1.9839	9399.80
1/256	3.0364E-05	1.9916	3.0365E-05	1.9916	3.0364E-05	1.9921	12000.9
EOC		2.00		2.00		2.00	

Figure 4.9, we demonstrate the absolute error surface (left panel) and errors comparison on nonuniform mesh (right panel). Figure (4.9)**(a)** represents the absolute error for two-dimensional case of Example 4.5.2 where $p(x) = 1$, $q(x) = 3 - \sin(2(x + y))$, $F(u) = \sin(u)$ within the domain $(x, y, t) \in [0, 10] \times [0, 10] \times [0, 1]$. In Figure (4.9)**(b)**,

we display the absolute error at $T = 1$ for Example 4.5.3 where $p(x) = 3 - \cos(2x)$, $q(x) = 3 - \sin(2x)$, $F(u) = u$ and $(\alpha_0, \alpha_1, \alpha_2) = (5/4, 23/20, 11/10)$. Figure (4.9)**(b)** shows the errors for nonsmooth exact solution by selecting $\theta = 3/2$ in Example 4.5.3 using various values of parameter γ. It can be observed from Figure (4.9)**(b)** that the error decreases when the nonuniform temporal meshes utilized in approximation method as compare to uniform mesh.

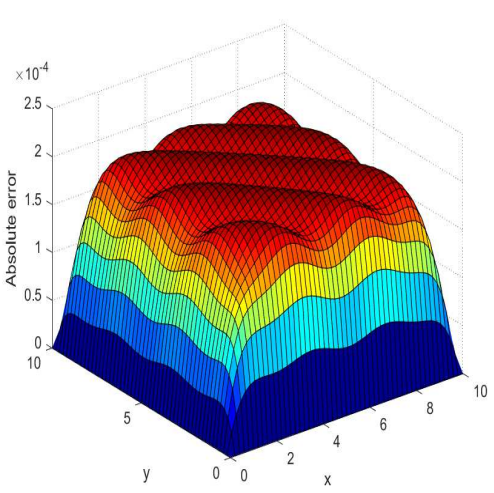

(a) For scheme (4.64)-(4.65) with $M_1 = M_2 = 50$, $N = 100$ and $\alpha = 1.25$.

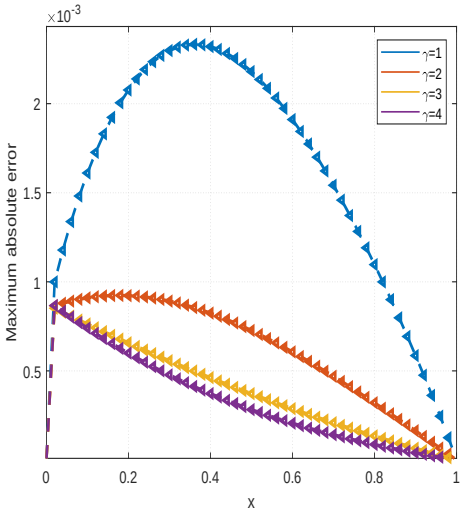

(b) For scheme (4.55) with $M = N = 100$ and $(\alpha_0, \alpha_1, \alpha_2) = (\frac{5}{4}, \frac{23}{20}, \frac{11}{10})$.

FIGURE 4.9: Graph of absolute errors on uniform (left) and nonuniform (right) time meshes for 2D case of Example 4.5.2 (left) and Example 4.5.3 (right).

Example 4.5.4. We examine the 2D Klein-Gordon and Sine-Gorden TFDW equation (4.1)-(4.3) within the domain $(x, y, t) \in [0, L_1] \times [0, L_2] \times [0, 1]$.

$$
\begin{cases}
{}^{C}\mathcal{D}^{\alpha}_{0,t} u(x,y,t) + q(x,y)F(u(x,y,t)) = \frac{\partial}{\partial x}\big(p(x,y)\frac{\partial u}{\partial x}\big) + \frac{\partial}{\partial y}\big(p(x,y)\frac{\partial u}{\partial y}\big) + f(x,y,t), \\
u(x,y,0) = \phi(x,y), \qquad u_t(x,y,0) = \varphi(x,y), \quad 0 \le x \le L_1,\ 0 \le y \le L_2, \\
u(0,y,t) = \Psi_1(0,y,t), \qquad u(L_1,y,t) = \Psi_2(L_1,y,t), \quad 0 \le y \le L_2, \quad 0 \le t \le T, \\
u(x,0,t) = \Phi_1(x,0,t), \qquad u(x,L_2,t) = \Phi_2(x,L_2,t), \quad 0 \le x \le L_1, \quad 0 \le t \le T.
\end{cases}
$$

Suppose that the exact solution to this test problem 4.5.4 is $u(x,y,t) = (t^{2\alpha} + t^{\psi})\sin(x)\sin(y)$. Then the corresponding source term has the form

$$f(x,y,t) = \frac{\Gamma(2\alpha+1)}{\Gamma(\alpha+1)}t^{\alpha} + \frac{(\psi+1)}{(\psi+1-\alpha)}t^{\psi-\alpha} + 2(t^{2\alpha}+t^{\psi})\sin(x)\sin(y) + q(x,y)F(u(x,y,t)).$$

We solve two-dimensional model 4.5.4 through the ADI scheme (4.64)-(4.66) on $\overline{\Omega}\times[0,T] = [0,2\pi]\times[0,2\pi]\times[0,1]$. Tables 4.17-4.20 display the maximum absolute errors and rate of convergence for 2D model in Example 4.5.4. In Table 4.17, we show the numerical results for the smooth exact solution by choosing $\psi = 2+\alpha$ with different choices of nonlinear term $F(u)$. In Tables 4.18-4.20, we represent the computational results for the nonsmooth exact solution by selecting $\psi = \alpha$ with $p(x,y) = 1$, $q(x,y) = 2-\sin(x+y)$ and different values of pair (α,γ). Tables 4.17, 4.18, 4.19 demonstrate the order of convergence and errors in time direction, setting $M_1 = M_2 = 100$ while varying N. Table 4.20 shows the OC and absolute errors in spatial direction with $N = 4000$ and varying the values of M_1, M_2. We can see that the numerical results are matched with EOC and the scheme gives good accuracy in both time and space directions.

TABLE 4.17: Temporal direction computational errors and convergence order for Example 4.5.4 with $\psi = (2+\alpha)$, $p(x,y) = 1$, $q(x,y) = 2 - \sin(x+y)$, $\alpha = 1.5$, and $h_1 = h_2 = \frac{1}{100}$ with domain $(L_1, L_2) = (2\pi, 2\pi)$.

	$F(u) = u$		$F(u) = \sin(u)$		$F(u) = u^3 - u$		
τ	$\|u^\tau - U^\tau\|_\infty$	OC	$\|u^\tau - U^\tau\|_\infty$	OC	$\|u^\tau - U^\tau\|_\infty$	OC	CPU(s)
1/8	1.2430E-01		1.0804E-01		1.3469E-01		0.842593
1/16	4.0042E-02	1.6343	3.8807E-02	1.4772	5.3249E-02	1.3388	2.799085
1/32	1.3967E-02	1.5195	1.3643E-02	1.5081	1.9838E-02	1.4245	8.512242
1/64	4.8601E-03	1.5230	4.7877E-03	1.5108	7.1865E-03	1.4649	26.62139
1/128	1.7166E-03	1.5014	1.7031E-03	1.4912	2.5876E-03	1.4737	87.89050
EOC		1.5		1.5		1.5	

TABLE 4.18: Temporal direction computational errors and convergence order for Example 4.5.4 with $\psi = \alpha$, $p(x,y) = 1$, $q(x,y) = 2 - \sin(x+y)$, $F(u) = u$, and $h_1 = h_2 = \frac{1}{100}$ with domain $(L_1, L_2) = (2\pi, 2\pi)$.

	$(\alpha,\gamma) = (1.5,1)$		$(\alpha,\gamma) = (1.5,3)$		$(\alpha,\gamma) = (1.8,2)$		
τ	$\|u^\tau - U^\tau\|_\infty$	OC	$\|u^\tau - U^\tau\|_\infty$	OC	$\|u^\tau - U^\tau\|_\infty$	OC	CPU(s)
1/16	3.9383E-02		1.6597E-01		2.1691E-01		1.9679
1/32	2.0517E-02	0.9407	4.4047E-02	1.9138	7.7008E-02	1.4940	7.7973
1/64	1.2601E-02	0.7032	1.2753E-02	1.7882	2.9913E-02	1.3643	25.894
1/128	8.5612E-03	0.5576	3.9733E-03	1.6824	1.2267E-02	1.2860	87.367
1/256	6.0910E-03	0.4911	1.3588E-03	1.5480	5.2110E-03	1.2351	317.57
EOC		0.5		1.5		1.2	

TABLE 4.19: Temporal direction computational errors and convergence order for Example 4.5.4 with $\psi = \alpha$, $p(x,y) = 1$, $q(x,y) = 2 - \sin(x+y)$, $F(u) = u^3 - u$, and $h_1 = h_2 = \frac{1}{100}$ with domain $(L_1, L_2) = (2\pi, 2\pi)$.

	$(\alpha,\gamma) = (1.5,1)$		$(\alpha,\gamma) = (1.5,3)$		$(\alpha,\gamma) = (1.8,2)$		
τ	$\|u^\tau - U^\tau\|_\infty$	OC	$\|u^\tau - U^\tau\|_\infty$	OC	$\|u^\tau - U^\tau\|_\infty$	OC	CPU(s)
1/32	2.4601E-02		1.9153E-01		1.1802E-01		6.9038
1/64	1.0750E-02	1.1944	4.6090E-02	2.0551	3.6403E-02	1.6968	31.272
1/128	7.4979E-03	0.5197	1.2063E-02	1.9339	1.2929E-02	1.4935	94.299
1/256	5.8816E-03	0.3502	3.4533E-03	1.8045	5.0251E-03	1.3633	315.58
1/512	4.5822E-03	0.3601	1.2024E-03	1.5221	2.0884E-03	1.2668	1199.2
EOC		0.5		1.5		1.2	

TABLE 4.20: Spatial direction computational errors and convergence order for Example 4.5.4 with $\Psi = \alpha$, $p(x,y) = 1$, $q(x,y) = 2 - \sin(x+y)$, $\tau = \frac{1}{5000}$, $(\alpha,\gamma) = (1.5,3)$ and different choices of $F(u)$ with domain $(L_1, L_2) = (2\pi, 2\pi)$.

	$F(u) = u^3 - u$		$F(u) = \sin(u)$		$F(u) = u$	
h	$\|u^\tau - U^\tau\|_\infty$	OC	$\|u^\tau - U^\tau\|_\infty$	OC	$\|u^\tau - U^\tau\|_\infty$	OC
1/8	1.7232E-02		2.6345E-02		2.3581E-02	
1/16	4.5451E-03	1.9227	6.6337E-03	1.9897	5.9569E-03	1.9850
1/32	1.1592E-03	1.9712	1.6691E-03	1.9907	1.5008E-03	1.9888
EOC		2.00		2.00		2.00

4.6 Conclusion

We constructed and analyzed two nonuniform difference schemes to compute the numerical solutions of the single-term and multi-term nonlinear TFDW equations with variable coefficients. The time-fractional derivative of order $\alpha \in (1,2)$ is approximated by half-point discretization process of nonuniform $L1$ formula. The nonuniform approximation methods have an advantage in solving the nonsmooth

solutions of the problem (4.1) over uniform grids. We employed the nonuniform $L1$ method to approximate Caputo derivative while the central difference formula is utilized for the spatial derivatives approximation, and then the given model (4.1)-(4.3) is transformed into an equivalent system of equations. The bound of error during the approximation of Caputo fractional derivative of order $\alpha \in (1,2)$ were also provided for both smooth and nonsmooth functions. The theoretical examination reveals that the proposed schemes (4.44), (4.55) and (4.64)-(4.66) exhibit the convergence rates $\mathcal{O}(N^{-\min(3-\alpha,\gamma(\alpha-1))}+h^2)$, $\mathcal{O}(N^{-\min(3-\alpha_r,\gamma(\alpha_r-1))}+h^2)$, $r=0,1,2$ and $\mathcal{O}(N^{-\min(3-\alpha,\gamma(\alpha-1))}+h_1^2+h_2^2)$, respectively. Numerical examples demonstrate that the derived schemes (4.44), (4.55) and (4.64)-(4.66) validate the order of convergence in both time and space directions. Furthermore, these schemes perform effectively in obtaining numerical solutions for nonsmooth case as well as two-dimensional problem (4.1). The examined numerical methods tackled the initial singularity at $t=0$ by using suitable choice of grading parameter γ. We provided numerous experiments with discontinuous initial conditions and smooth, nonsmooth exact solutions to attain the optimal accuracy of the presented schemes.

****